The Role of IFNγ in the Immune Pathogenesis of Primary Sclerosing Cholangitis

Dissertation

Zur Erlangung der Würde des Doktors der Naturwissenschaften
des Fachbereichs Biologie, der Fakultät für Mathematik, Informatik und Naturwissenschaften,
der Universität Hamburg

vorgelegt von

Gevitha Ananthavettivelu, geb. Ravichandran

Aus Quierschied

Hamburg 2019

Tag der Disputation: 29.05.2020

Vorsitzende der Disputation

Prof. Dr. Julia Kehr
Universität Hamburg
Institut für Pflanzenwissenschaften und Mikrobiologie

Gutachter der Disputation

Prof. Dr. Gisa Tiegs
Universität Klinikum Hamburg-Eppendorf
Institut für Experimentelle Immunologie und Hepatologie

Jun.-Prof. Dr. Wim Walter
Universität Hamburg
Institut für Pflanzenwissenschaften und Mikrobiologie

Gutachter der Dissertation

Prof. Dr. Gisa Tiegs
Universität Klinikum Hamburg-Eppendorf
Institut für Experimentelle Immunologie und Hepatologie

Prof. Dr. Thomas Dobner
Heinrich-Pette-Institut
Abteilung für Molekulare Virologie

Table of contents

Declaration of own contribution to presented published work

The data shown in this thesis have already been published in the JOURNAL OF HEPATOLOGY as “Interferon-γ-dependent immune responses contribute to the pathogenesis of sclerosing cholangitis in mice” by Gevitha Ravichandran, Katrin Neumann, Laura Berkhout, Sören Weidemann, Annika E. Langeneckert, Dorothee Schwinge, Tobias Poch, Samuel Huber, Birgit Schiller, Leonard U. Hess, Annerose E. Ziegler, Karl J. Oldhafer, Roja Barikbin, Christoph Schramm, Markus Altfeld and Gisa Tiegs. The publication is the result of a collaborative effort to which I substantially contributed in the planning and performing of experiments, analysis and interpretation of data as well as statistical analysis. The following delineates my contributions and those of my colleagues.

Gisa Tiegs and Roja Barikbin planned this study and obtained funding. Sören Weidemann analyzed the hematoxylin and eosin staining. I planned and performed the experiments. In complex and time-consuming experiments, I was supported by Laura Berkhout, Annika E. Langeneckert, Dorothee Schwinge, Tobias Poch, Birgit Schiller, Leonard U. Hess and Annerose E. Ziegler. Karl J Oldhafer, Markus Altfeld and Christoph Schramm enabled the access to human samples. Samuel Huber and Christoph Schramm supported this study with supply of mice. I analyzed and interpreted the data under the supervision of Roja Barikbin, Katrin Neumann and Gisa Tiegs. The manuscript was drafted by Gisa Tiegs and Katrin Neumann. All authors were involved in the critical revision of the manuscript.

Hamburg, 22.6.2020

Place and date

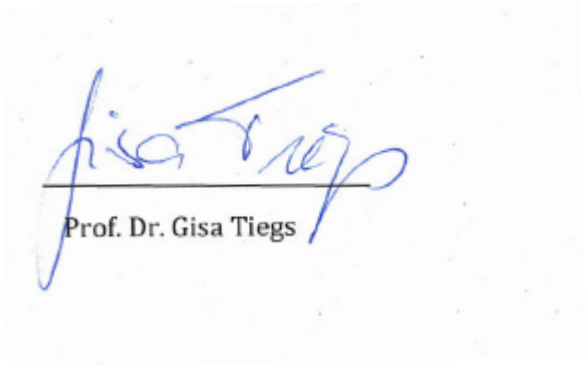

List of publications

Journal articles

- Ravichandran G, Neumann K, Berkhout L, Weidemann S, Langeneckert AE, Schwinge D, Poch T, Huber S, Schiller B, Hess LU, Ziegler AE, Oldhafer KJ, Barikbin R, Schramm C, Altfeld M, Tiegs G. Interferon-γ-dependent immune responses contribute to the pathogenesis of sclerosing cholangitis in mice. J Hepatol. 2019;71(4):773–82
- Berkhout L, Schiller B, Ravichandran G, Krech T, Sass G, Tiegs G Barikbin R. Deletion of tumour necrosis factor alpha receptor 1 elicits an increased TH17 immune response in the chronically inflamed liver. Sci Rep. März 2019;9(1):4232.
- Langeneckert AE, Lunemann S, Martrus G, Salzberger W, Hess LU, Ziegler AE, Poch T, Ravichandran G, Matschl U, Bosse JB, Tiegs G, Fischer L, Koch M, Herkel J, Oldhafer KJ, Schramm C, Altfeld M. CCL21-expression and accumulation of CCR7+ NK cells in livers of patients with primary sclerosing cholangitis. Eur J Immunol. 2019 Feb 20
- Lunemann S, Langeneckert AE, Martrus G, Hess LU, Salzberger W, Ziegler AE, Lobl SM, Poch T, Ravichandran G, Sauter J, Schmidt AH, Schramm C, Oldhafer KJ, Altfeld M, Korner C. Human liver-derived CXCR6(+) NK cells are predominantly educated through NKG2A and show reduced cytokine production. J Leukoc Biol. Juni 2019;105(6):1331–40.

Congress poster presentations

- Ravichandran G, Tiegs G, Barikbin R. The Role of IFNγ in the Immune Pathogenesis of Primary Sclerosing Cholangitis. Z Gastroenterol. 2016;54(12):A1.34.
- Ravichandran G, Krech T, Tiegs G, Barikbin R. The Role of IFNγ in the Immune Pathogenesis of Primary Sclerosing Cholangitis. Z Gastroenterol. 2018;56(01):A1.12.
- Berkhout L, Schiller B, Ravichandran G, Krech T, Sass G, Tiegs G, u. a. Deletion of tumor necrosis factor α receptor 1 leads to increased tissue damage and fibrosis in the chronically inflamed liver. Z Gastroenterol. 2018;56(01):A1.10.
- Ravichandran G, Neumann K, Berkhout L, Weidemann S, Schwinge D, Schramm C, u. a. Interferon-γ-dependent immune responses contribute to the pathogenesis of primary sclerosing cholangitis in mice. Z Gastroenterol. 2019;57(01):P2.30.
- Ravichandran G, Neumann K, Berkhout L, Weidemann S, Langeneckert AE, Schwinge D, Poch T, Huber S, Schiller B, Hess LU, Ziegler AE, Oldhafer KJ, Barikbin R, Schramm C, Altfeld M, Tiegs G. Interferon-γ promotes CD8 T cell and NK cell cytotoxicity and fibrosis in *Mdr2*$^{-/-}$ mice. 48th annual Conference of the German Society of Immunology, 2019, München

Congress oral presentations

- Ravichandran G, Krech T, Tiegs G, Barikbin R. The role of IFNγ in the immune pathogenesis of primary sclerosing cholangitis. 47th annual Conference of the German Society of Immunology, 2017, Erlangen

List of Abbreviations

Ab	antibody
ad	fill-up to
AD	Autoimmune disease
AIH	autoimmune hepatitis
ALD	alcoholic liver disease
ALT	alanine aminotransferase
ANOVA	analysis of variance
APC	antigen-presenting cell
AP	alkaline phosphatase
AST	aspartate transaminase
BA	bile acids
bp	base pairs
BSA	bovine serum albumin
cDNA	copy DNA
CIA	collagen-induced arthritis
Col3a1	collagen type III α 1 chain
Ct	threshold cycle
DAMP	damage-associated molecular pattern
DC	dendritic cell
DR5	death receptor 5
dNTP	deoxynucleosidtriphosphate
EAE	experimental autoimmune encephalomyelitis
ECM	extracellular matrix
EDTA	ethylenediaminetetraacetic acid
ELISA	enzyme-linked-immunosorbent assay
FCS	fetal calf serum
FITC	fluorescein isothiocyanate
Foxp3	forkhead box p3
g	gram
gGT	g- glutamyltransferase
GzmB	gramzyme B
h	hours
H&E	haematoxylin & eosin
HCC	hepatocellular carcinoma
HLA	human leukocyte antigens
HSC	hepatic stellate cell
IBD	inflammatory bowel disease
IFNs	interferons
Ig	immunoglobulin
IL	interleukin
ILC	innate lymphoid cell
i.p.	intraperitoneal
IRF1	interferon regulatory factor 1
i.v.	intravenous
JAK	janus kinase
KC	kupffer cell
kDa	kilo dalton

ko	knockout
LPS	lipopolysaccharide
LSEC	liver sinusoidal endothelium cell
mHAI	modified hepatitis activity index
Mdr2	multidrug resistance protein 2
mg	milligram
MHC	major histocompatibility complex
min	minute
mL	millilitres
MRCP	magnetic resonance cholangiopancreatography
mRNA	messanger ribonucleic acid
NAFLD	nonalcoholic fatty liver disease
NASH	non-alcoholic steatohepatitis
neutrophil	neutrophil granulocyte
NF-κB	nuclear factor κ-light-chain-enhancer of activated B cell
NK cell	natural killer cell
NKT cell	natural killer T cell
NPC	non-parenchymal cell
PBC	primary biliary cholangitis
PC	phosphatidylcholine
PCR	polymerase chain reaction
PRR	pattern recognition receptor
PSC	primary sclerosing cholangitis
qRT-PCR	quantitative real time PCR
RA	rheumatoid arthritis
ROS	reactive oxygen species
rpm	rounds per minute
RT	room temperature
SLE	systemic lupus erythematosus
SEM	standard error of the mean
STAT	signal transducer and activator of transcription protein
TCR	T cell receptor
TGFβ	tumor growth factor β
Th cell	T helper cell
TLR	toll-like receptor
TNF	tumor necrosis factor
TRAIL	tumor necrosis factor-related apoptosis-inducing ligand
Tregs	regulatory T cells
U	units
UKE	University hospital Hamburg-Eppendorf
WT	wild-type

List of Tables

List of Figures

1. Introduction

Chronic liver diseases are currently one of the major causes of increased morbidity and mortality worldwide (1). Genetic predisposition as well as exogenous factors like inadequate nutrition, abuse of alcohol or drugs and viral infection cause liver injury, which in the worst case scenario is followed by scarring and liver failure. Examples of chronic liver diseases are amongst others autoimmune hepatitis (AIH), alcoholic liver disease, non-alcoholic fatty liver disease, primary biliary cholangitis (PBC) and primary sclerosing cholangitis (PSC). Due to the complexity of the pathophysiology no adequate treatment is available so far, which clearly emphasizes the need for understanding the underlying mechanisms driving disease pathogenesis.

Some chronic liver diseases such as AIH, PBC and PSC are discussed as autoimmune diseases, since T cells and autoantigens were suspected to be involved in immune pathogenesis. According to a publication in 1974 (2), autoimmune diseases were stated to be caused by interferons and to benefit from anti-cytokines therapies. Since then, many studies revealed anti-cytokine therapy to be useful in different approaches; anti-IFNγ treatment especially was observed to be highly effective in Th1-mediated autoimmune diseases such as inflammatory skin diseases, rheumatoid arthritis (RA) and type I diabetes (3).

PSC, the chronic liver disease this work is focused on, is described by its increased accumulation of T cells and enhanced production of IFNγ and IFNγ-inducible chemokines (4–6). Therefore, it has been assumed that the pleiotropic cytokine IFNγ plays a role in the immune pathogenesis of PSC and this question will be addressed in the following thesis. This chapter will first introduce to the physiology and pathophysiology of the liver, give an overview of PSC and the immune cells possibly involved in its pathogenesis.

1.1. The liver and its function

The liver is the largest solid organ in the human body and encompasses various functions. Besides bile production and the metabolism of fat and carbohydrates, the liver also participates in the degradation of erythrocytes, detoxification of the blood and synthesis of plasma proteins. Hormone production and immunological functions are additional characteristics of the liver (7,8). Not only is the diversity of its functions impressive, but

also the liver's unique ability to regenerate even after a loss of 75% of its tissue is remarkable (9).

In comparison to other organs the liver receives a dual blood supply. About 80% of the blood comes from the portal vein with high concentrations of dietary antigens and bacterial products and a low oxygen content. The remaining 20% is instead obtained from the hepatic artery, which is rich in oxygen (10).

The liver is divided into four lobes, namely the left lobe (lobus hepatis sinister), the right lobe (lobus hepatis dexter), the caudate lobe (lobus caudatus), and the quadrate lobe (lobus quadratus) (11). The liver parenchyma is further divided into functional units called hepatic lobules consisting of hepatocytes organized in irregular radiating columns around small blood vessels called sinusoids (8,11). The liver sinusoidal endothelial cells (LSECs), a monolayer of fenestrated liver endothelial cells, line the sinusoids. The portal triad, consisting of the hepatic artery, the portal vein and the intralobular bile duct, is located at the end of every liver lobule. The liver-resident macrophages, referred to as Kupffer cells that perform phagocytosis and clearance with immune-regulatory ability, are in direct contact with the LSECs. In addition, the space between the LSECs and hepatocytes, called space of Disse, harbors the hepatic stellate cells, which regulate storage of vitamin A and extracellular matrix deposition in case of liver injury (8)(Fig.1).

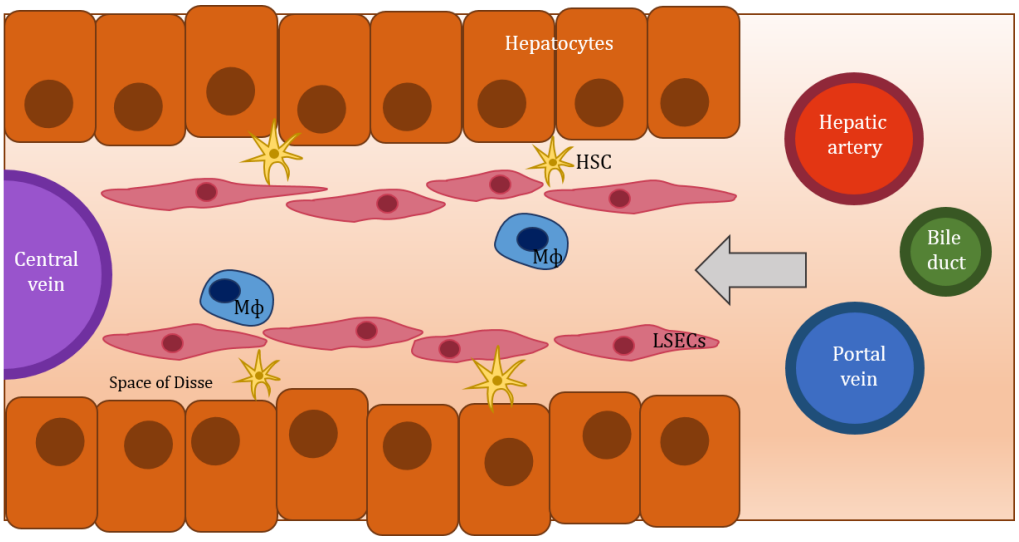

Fig. 1: Schematic overview of the liver lobule. The blood coming from the portal vein and hepatic artery drains through the sinusoids to the central vein. Hepatocytes are organized around the sinusoids, while LSECs line them and are in direct contact to Kupffer cells (Mϕ). The space between hepatocytes and LSECs is populated by HSCs. LSECs: liver sinusoidal endothelial cells; HSCs: hepatic stellate cells.

1.2. Enterohepatic circulation

As the largest gland in the body, the liver is responsible for the production of bile, a digestive fluid comprised of bile acids (BA), phospholipids, electrolytes, cholesterol and bilirubin. Especially the BA are critical for the solubilization of lipolytic products, cholesterol and fat-soluble vitamins (7,12). Besides its digestive functions, bile is also involved in the excretion processes of endogenous and exogenous compounds such as bilirubin, cholesterol, drugs and toxins out of the body via enterohepatic circulation. This cycle describes the transportation of BA and other products from the gut to the liver and *vice versa* via portal circulation (Fig. 2).

Generally, BA excreted by hepatocytes into the bile canaliculi are drained into the bile ductules of the portal tract via the canal of Hering (10) and stored in the gallbladder after conjugation with taurine (mice) or glycine (humans). Following food intake, the BA are secreted into duodenum to aid digestion and for cholesterol and lipid metabolisms. 95% of the BA are reabsorbed at the distal ileum, while the remaining 5% are deconjugated and further metabolized into secondary BA (13). The next step is the colonic reabsorption and transportation of the secondary BA to the liver for conjugation purposes. Unabsorbed secondary bile acids are finally excreted via the colon by the host (14).

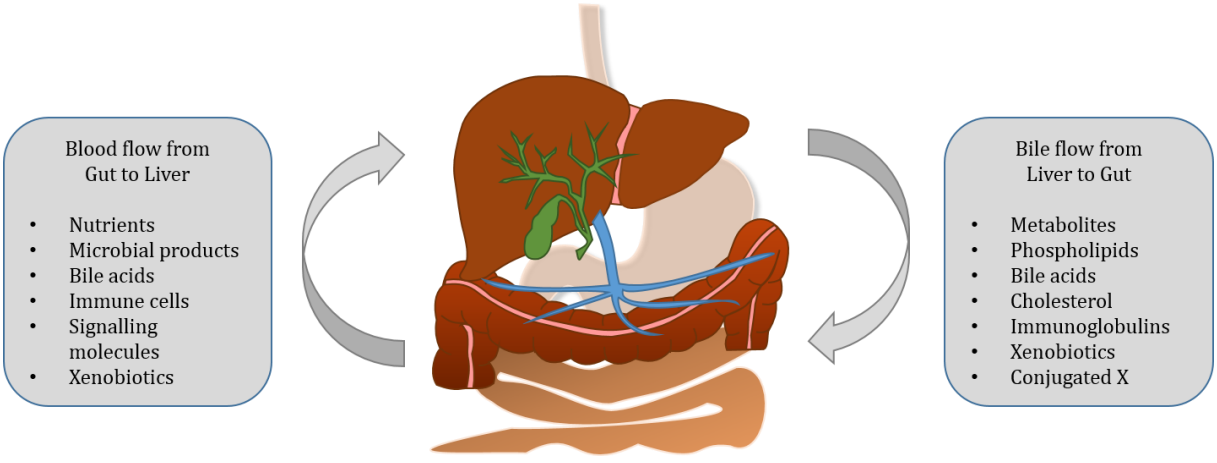

Fig. 2 The enterohepatic circulation. The enterohepatic circulation describes the transportation of BA and other factors from the gut to the liver and *vice versa* via portal circulation. While predominantly metabolites, BA and cholesterol enter the intestine from the liver, BA, nutrients and microbial products are mainly transported from the gut to the liver. BA: bile acids.

Disturbances in the circulatory pathway leading to altered bile homeostasis are strongly associated with clinical manifestations ranging from cholestasis to diarrhea (7). One such disturbance can occur in response to microbial dysbiosis for example, which describes a microbial imbalance or maladaptation in the human body. Levels of primary BA synthesis

and the production of secondary BA are regulated by the gut microbiota, which has co-metabolic functions in bile homeostasis (15,16). In general, microbiota are described as extremely diverse communities of microorganisms comprised of bacteria, archaea, eukaryotes and viruses (17). They are not only involved in the generation of metabolites and hormones, which act on the gut function and control indirectly the function of extra-intestinal organs such as the liver (1), but also in the bidirectional communication between the intestine and the liver. While the microbiota are able to influence the development and function of the host immune system, the immune system has the capacity to shape microbiota composition and diversity in the gut (1).

Due to the high relevance of gut microbiota in host functionality, maintaining well-balanced gut microbiota is essential (1). Any alteration in the microbial composition will accordingly have an impact on host physiology. Several studies have already shown that intestinal dysbiosis is involved in the pathophysiology of chronic diseases (1,16). Primary sclerosing cholangitis is such a chronic disease, described as being triggered among other causes by dysfunctional gut microbiota (18).

1.3. Primary sclerosing cholangitis

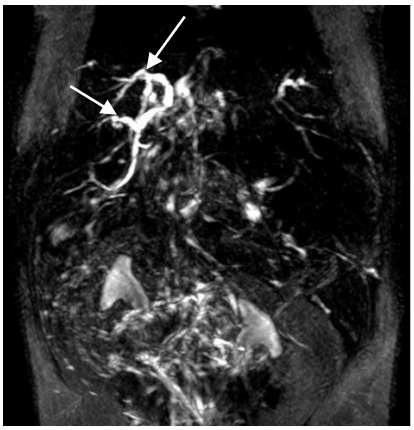

Fig. 3 Visualization of biliary structuring by magnetic resonance cholangiopancreatography (MRCP).

Primary sclerosing cholangitis (PSC) is a chronic cholestatic liver disorder, characterized by multi-focal bile duct strictures and progressive, biliary inflammation and fibrosis (15,19,20). In general, PSC progresses slowly over a long period of time from biliary inflammation to fibrosis and cirrhosis, finally resulting in liver failure (19). Liver transplantation is currently the only option as a cure, since no adequate treatment is available (15,20). However, recurrence has also been reported in several cases, which emphasizes how little the underlying mechanism in PSC development is currently understood (15).

PSC is strongly associated with inflammatory bowel disease (IBD), with increased incidence of ulcerative colitis. It also acts as a high risk factor for colon, bile-duct and gallbladder cancers and cholangiocarcinoma (15,19,20).

Despite a lack of symptoms in 40-50% of PSC patients at the beginning of disease progression, patients develop symptoms like hepatomegaly, splenomegaly, abdominal pain, pruritus, jaundice and fatigue as well as weight loss, episodes of fever and chills over time (19–21). Males (ratio 2:1) at a mean age of 40 years have been predominantly diagnosed with PSC (19,20). Diagnosis occurs based on serological and histological analyses and cholangiography, commonly MRCP (magnetic resonance cholangio-pancreatography) (Fig. 3). Generally, PSC patients exhibit elevated activities of the liver enzymes alkaline phosphatase (AP), γ-glutamyltransferase (γGT), alanine transaminase (ALT) and aspartate transaminase (AST). Serum bilirubin is usually not enhanced at the time of diagnosis, but rises with advanced disease progression, acting as a hint for cholestasis (21). However, these parameters are only indications for liver inflammation and not specific for PSC.

1.4. Pathogenesis of PSC

Even though the etiology of PSC is still unknown, involvement of genetic and environmental risk factors have been proposed (19,20). Genome-wide association studies have found around 22 risk loci to be associated with PSC and most of them were linked to autoimmune diseases and IBD (22). Both risk factors are believed to initiate the pathophysiology of PSC by inducing microbial dysbiosis in the intestine, resulting in increased intestinal permeability ("leaky gut") and bacterial translocation into the liver via portal circulation (1,23). While gut-derived factors promote activation of hepatic innate immune cells by binding to toll-like receptors (TLRs) for example, gut-derived antigens trigger adaptive immune responses following presentation by antigen-presenting cells (APCs). In addition, migration of activated gut-derived T cells into the liver is proposed to initiate immune-mediated damage by interacting with biliary epithelial cells and promoting disruption of tight junctions (15,20).

Dysregulation of bile homeostasis in response to microbial dysbiosis is also suspected to activate cholangiocytes due to failed protection against BA and to subsequently produce pro-inflammatory cytokines such as TNFα, IL-6 and, IL-8 and initiate recruitment of further immune cells to the inflamed tissue. The interaction of the activated cholangiocytes with recruited immune cells such as T cells, natural killer (NK) cells, neutrophils as well as macrophages and other resident cells finally foster biliary inflammation (15)(Fig. 4).

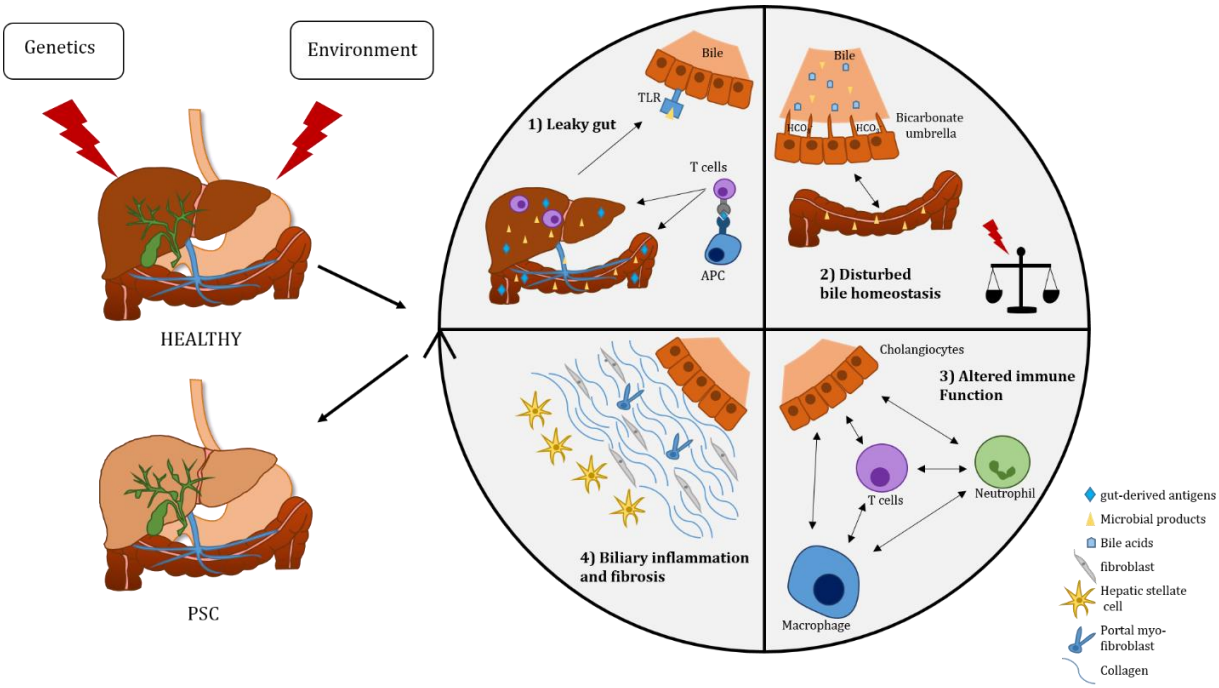

Fig. 4 Overview of the pathophysiology of primary sclerosing cholangitis (PSC). This schema illustrates clockwise the postulated development of PSC. Genetic and environmental factors are believed to induce microbial dysbiosis resulting in a leaky gut. **(1)** Via the portal circulation gut-derived antigens and microbial products reach the liver and trigger immune responses. Moreover, activated T cells are assumed to migrate from the intestine to the liver inducing immune-mediated damage. **(2)** Mechanisms such as bicarbonate umbrella protect cholangiocytes from BA-toxicity. But in PSC defective protection leads to microbial infection of the bile and altered bile homeostasis. **(3)** Following activation cholangiocytes trigger the recruitment and activation of additional immune cells like T cells, neutrophils and macrophages fostering biliary inflammation. **(4)** Crosstalk of hepatic stellate cells and portal myofibroblasts with cholangiocytes finally promote the development of chronic liver fibrosis.

Ultimately, persistent hepatic inflammation promotes the development of obliterative chronic fibrosis. Technically, liver fibrosis is considered a wound-healing mechanism in response to liver injury. Due to persistent death of epithelial cells, the inflammatory machinery orchestrates the activation and transdifferentiation of hepatic stellate cells to myofibroblasts. These cells produce increased amounts of extracellular matrix (ECM) proteins including collagen, leading to scar formation. Although fibrosis is self-limiting in acute liver injury, in the case of chronic inflammation, scarring proceeds in an uncontrolled and excessive manner (24), resulting in distorted liver architecture. Fibrosis slowly progresses to biliary cirrhosis, which is characterized by the development of nodules of regenerating hepatocytes and by blockage of blood flow, which results in hepatic insufficiency and portal hypertension (25). While fibrosis can be reversed by eliminating the cause, in case of cirrhosis the possibilities are limited and associated with complications and at some stage it is even irreversible. Subsequently, cirrhosis can lead to the development of hepatocellular carcinoma (HCC) or cholangiocarcinoma for example (Fig. 5).

Nevertheless, the processes described here as leading to the pathogenesis of PSC are not fully understood, since some findings contradict the theory. Neither application of immunosuppressive drugs pre- and post-liver transplantation under the assumption that PSC is an autoimmune disease (AD), nor colectomy in order to prevent bacterial translocation from the gut and ursodeoxycholic acid administration to treat cholestasis, had ameliorative effects on the progression of PSC (15). Even if the lack of success might be caused by an inadequate choice of time point or drug concentration (15), the need for a better understanding of the pathophysiology is unquestionable.

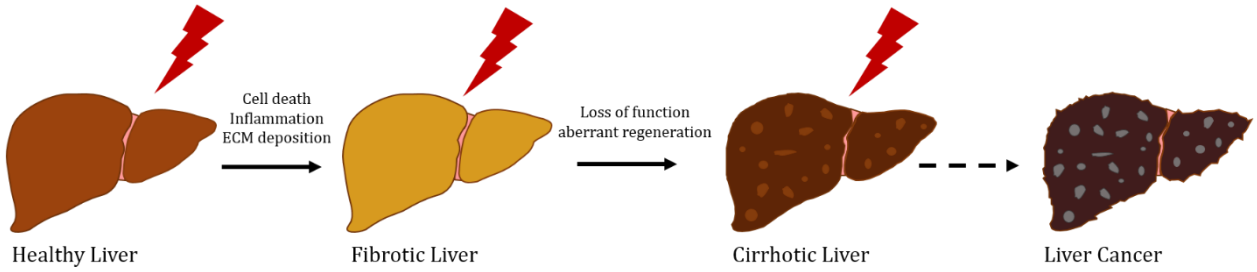

Fig. 5: Initiation and progression of chronic liver injury. Challenges to the liver lead to the development of chronic liver injury. It is characterized by increased cell death, especially of hepatocytes and cholangiocytes, fostering inflammatory responses by secretion of pro-inflammatory mediators and recruitment of immune cells to the site of injury. Upon activation hepatic stellate cells transdifferentiate to myofibroblasts producing extracellular matrix proteins and inducing scar formation. Excessive ECM deposition and formation of regeneration nodules describes the cirrhotic liver with loss of function. Persistent progression of cirrhosis favors the development of liver cancer.

1.5. Immune-mediated biliary disease

Even though the pathophysiology of PSC is controversial, it is generally accepted to be an immune-mediated biliary disease. First hints were obtained from genomic-wide association studies, when increased up-regulation of the human leukocyte antigens (HLA) on chromosome 6p21 was observed in PSC patients. This gene, encoding the major histocompability complex (MHC), is known to be involved in the process of antigen presentation and subsequently in the activation of adaptive immunity and in particular of T cells. Additional genes found to be associated with PSC were linked to T cell activation and development (26), pinpointing a possible involvement of T cells in immune pathogenesis (27). Further studies have linked PSC to dysregulated apoptosis of activated $CD4^+$ T cells (28) and to altered function of regulatory T cells (29), further supporting T cell participation in disease progression. Another clue was the increased accumulation of T cells with a bias towards type 1 T helper cells (Th1 cells) around the bile ducts and portal tracts in PSC patients (30,31). Based on these data, T cells are suspected to play an important part in the immune pathogenesis of PSC.

Besides elevated levels of the IFNγ-induced chemokines CXCL9, CXCL10 and CXCL11 in the sera of PSC patients (5,6), hepatic gene expression of *Cxcl9*, *Cxcl10*, and the IFNγ-specific transcription factors *Stat1* and *Irf1* (32) also directed the focus towards Th1 cells as an effector cell population, that might drive PSC, with IFNγ as their effector cytokine.

1.6. The pleiotropic cytokine IFNγ

Interferons (IFNs) belong to the family of structurally related cytokines with antiviral capacities. They fulfil a multitude of functions including antitumor activity and immunomodulation. IFNs are subdivided in type I, type II and type III IFNs according to receptor specificity and sequence homology (33). The interaction between ligand and receptor initiates primarily the JAK-STAT signaling pathway resulting in the expression of IFN-inducible genes. In this study, the focus is on IFNγ, which is the exclusive member of type II IFNs.

IFNγ acts as a central mediator of the adaptive immune response against pathogens (34). As one of the most potent pleiotropic cytokines (35), IFNγ exerts numerous functions including activation of macrophages by promoting antigen processing, presentation, and microbicidal effector functions. It is additionally involved in antiviral response, inhibition of cellular proliferation, induction of apoptosis, and leukocyte trafficking (33). Furthermore, it plays a role in the regulation of growth, maturation, and differentiation of many cell types such as NK cell activity, promotion of Th1 cells and cytotoxic CD8+ T cell development (33). In general, IFNγ is essential in perpetuating inflammation and Th1 responses, whereby the differentiation of regulatory T cells, Th2 cells and Th17 cells is inhibited (34).

However, aberrant IFNγ expression has been strongly associated with AD. Chronic exposure to this cytokine leads to ADs such as systemic lupus erythematosus (SLE) or rheumatoid arthritis (RA) (3,34,36). The up-regulation of MHCII expression as a result of increased IFNγ production was presumed to be important in the course of collagen-induced arthritis (CIA) and RA (37). Additionally, mouse models of CIA and experimental autoimmune encephalomyelitis (EAE) have depicted an involvement of IFNγ in disease progression (34).

Although IFNγ was initially suspected to predominantly act as a pro-inflammatory cytokine, studies have shown that it fulfils bidirectional immunoregulatory functions.

Besides the promotion of inflammation, IFNγ also assumes protective and anti-inflammatory functions such as inhibition of T cell proliferation and of neutrophil mobilization, stimulation of regulatory T cells and inhibition of Th17 response (36). While an application of IFNγ at the early stage of EAE aggravated disease progression, at a later stage of the disease, the administration reduced the severity of EAE by suppressing Th17 response (38). In models of autoimmune nephritis and myocarditis endogenous IFNγ have also revealed protective effects (36). Accordingly, the functions of IFNγ in disease progression have to be determined in each model and stage individually.

1.7. Immune cells linked to IFNγ

The major IFNγ-producing immune cell populations are $CD4^+$ T cells, $CD8^+$ T cells, NKT cells, $\gamma\delta^+$ T cells and NK cells (33). While the T cell populations mentioned are part of adaptive immunity, NK cells belong to the innate immune system. In addition to IFNγ-producing cell populations, there are immune cells which are activated by this cytokine including macrophages. Due to the high complexity of this subject, this thesis only focuses on the immune cells stated earlier ($CD4^+$ T cells, $CD8^+$ T cells, NKT cells, $\gamma\delta^+$ T cells and NK cells) with the aim of analyzing the involvement of IFNγ and IFNγ-producing effector cell populations in the disease progression of PSC.

CD4+ T cells are mainly involved in cell-mediated immunity and release a variety of mediators following activation, which allow the shaping of immune responses. Basically, after recognition of foreign antigens presented by MHC class II molecules on professional APCs, $CD4^+$ T cells are activated and induce the differentiation of naïve T cells to specific T helper cell subtypes depending on the local cytokine milieu (Th1, Th2, Th9, Th17 and Treg). Each subtype differs by their functions, distinct expression of transcription factors and production of effector cytokines. Th1 cells initiate cell-mediated cytotoxic response and are characterized by their expression of the key transcription factor *Tbx21* and by their production of IFNγ (39). **CD8+ T cells** are described by their strong cytotoxic potential against tumor cells, viruses, bacteria and intracellular pathogens. After recognition of its antigen presented by MHC class I molecule, CD8+ T cells release cytokines such as IL-2 and IFNγ in response and exert their cytotoxicity by initiating Fas or perforin/granzyme B pathways for instance (40). **Natural killer T (NKT) cells** are a heterogeneous subtype of T cells expressing T cell and NK cell markers. In contrast to T cells, they recognize non-peptide antigens presented by CD1d molecules and produce

cytokines such as IFNγ, IL-4 as well as IL-10. Furthermore, they induce cell death via death receptors or the release of cytolytic granules (41,42). **γδ T cells** are a very small subset of unconventional T cells expressing T cell receptors (TCRs) composed of γ and δ chains, unlike TCR $\alpha\beta^+$ $CD4^+/CD8^+$ T cells. They recognize infected cells and thereupon produce cytokines and chemokines and induce apoptosis in target cells (43). **Natural killer (NK) cells** belong to the group of innate lymphoid cells (ILCs), which are defined by the lack of antigen-specific receptors. Elimination of aberrant cells is their primary task. In order to fulfil this duty, NK cells store cytolytic granules, which are released in contact with target cells. Moreover, they are potent producers of IFNγ (44,45).

In this context, the increased ability of IFNγ-producing cells to exert cytotoxic functions as well is noticeable. The cytotoxic potential of these cells can be measured by the expression of tumor necrosis factor-related apoptosis-inducing ligand (TRAIL) and granzyme B (GzmB), for instance. TRAIL is a pro-apoptotic molecule expressed on the surface of NK cells and CD8+ T cells, which is capable of interacting with the TNF receptor family, also called death receptors, on target cells and inducing apoptosis (46). Like TRAIL, granzyme B is a cytotoxic molecule, which is produced in the granules of NK cells and cytotoxic T cells. It is released along with perforin, which facilitates the entry of granzymes into the target cells. Subsequently, the granzymes cleave a variety of targets such as caspases resulting in apoptosis of target cells (47). CD107a on the other hand, is a degranulation marker, which is transported to the surface after activation of NK cells and CD8+ T cells. It is accepted as an indirect marker for cytotoxicity (48).

In contrast to the other immune cells, **macrophages** do not produce IFNγ, but are rather activated by this cytokine. In case of injury, macrophages acquire microbicidal effector functions upon activation and eliminate pathogens by phagocytosis or release of toxic metabolites (33). In addition, they secrete pro-inflammatory cytokines inducing recruitment of immune cells to the site of injury. Activation by IFNγ also enhances anti-tumor functionality of macrophages and up-regulates antigen processing and presentation capabilities. Moreover, the activation by IFNγ leads to a shift towards M1 phenotype, which is described as pro-inflammatory (49).

1.8. Multidrug resistance protein 2 knockout mice – mouse model for PSC

A suitable mouse model for the analysis of PSC are the multidrug resistance protein 2 knockout (*Mdr2*$^{-/-}$) mice. Biliary inflammation, ductular proliferation and onion skin type periductal fibrosis are characteristics which were observed in *Mdr2*$^{-/-}$ mice as well as in PSC patients, encouraging their use in this study (50–52). This is additionally supported by the mutation of the human orthologue MDR-3, which was also found in PSC patients (53).

Mdr2 (Abcb4) is a floppase exclusively expressed in the liver that translocates phosphatidylcholine (PC) from the inner to the outer leaflet of the canalicular membrane of the hepatocyte (54). One of the main functions of the Mdr2 p-glycoprotein is the maintenance of phospholipid concentration in bile and the protection of the biliary tract from harmful bile acids by forming micelles, which consist of cholesterol, BA and PC (55). Absence of this transporter results in increased accumulation of detrimental bile acids in the bile, causing membrane damage and cell death of hepatocytes (Fig. 6). Ongoing destruction of epithelial cells promotes portal inflammation and bile duct proliferation (55).

Within the first weeks of age *Mdr2*$^{-/-}$ mice develop progressive hepatitis and portal inflammation, followed by enhanced storage of connective tissue leading to fibrosis. As a consequence of chronic inflammation and progressive fibrosis, *Mdr2*$^{-/-}$ mice have been shown to develop HCC within 12 to 15 months of age (51,52).

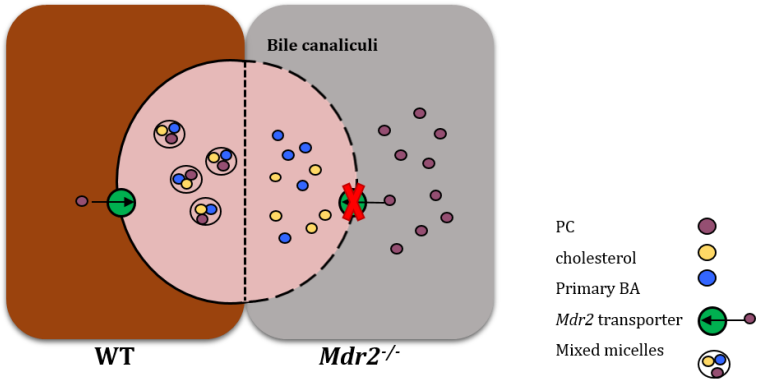

Fig. 6 Multidrug resistance protein 2 knockout mouse. Mdr2 (Abcb4) is a floppase transporting PC from the inner to the outer leaflet of the canalicular membrane of the hepatocyte. Lack of Mdr2 protein leads to membrane destruction and cell death of hepatocytes due to impaired BA-protection and finally to chronic liver inflammation. Phosphotidylcholine (PC), bile acids (BA).

1.9. Aim of the study

PSC is an idiopathic, chronic cholestatic liver disorder characterized by biliary inflammation and fibrosis. PSC patients exhibit an increased accumulation of IFNγ-producing Th1 cells around the bile ducts and have enhanced levels of the IFNγ-induced chemokines CXCL9 and CXCL10 in the sera, indicating an involvement of IFNγ in the immune pathogenesis of PSC. The aim of this study was to analyze the role of IFNγ as well as IFNγ-producing or -activated cells in disease progression. Therefore, *Mdr2*$^{-/-}$ mice which develop progressive cholangitis, ductular proliferation and periportal fibrosis (51,52) were used as mouse models due to their resemblance to human PSC.

Following analysis of IFNγ production in *Mdr2*$^{-/-}$ mice in comparison to C57BL/6 WT mice, the immune cells found to produce IFNγ were depleted one by one in the *Mdr2*$^{-/-}$ mice in order to investigate the contribution of the different cell populations to biliary inflammation and liver fibrosis. Additionally, *Mdr2*$^{-/-}$ x *IFNg*$^{-/-}$ mice were generated in order to analyze the impact of IFNγ on the pathogenesis and its functions. Moreover, explant livers from PSC patients and control patients were analyzed with regard to lymphocytic composition in PSC in order to find the major culprits leading to PSC. The control liver samples were obtained from patients undergoing liver resection due to tumor metastases.

2. Material and Methods

2.1. Materials

2.1.1. Technical Equipment

Table 2-1 Technical Equipment

Equipment	Supplier
BD FACSCanto™ III	BD Biosciences, Franklin Lakes
BD LSR Fortessa™	BD Biosciences, Franklin Lakes
Bio-Plex 200 analyzer	Bio-Rad Laboratories, Hercules
BZ-9000 microscope	Keyence, Neu-Isenburg
Centrifuge 5417R	Eppendorf, Hamburg
Centrifuge 5810R	Eppendorf, Hamburg
Clean Bench Hera cell 240	Thermo Fisher Scientific, Hamburg
Clean Bench, MSC advantag	Thermo Fisher Scientific, Hamburg
COBAS Integra® 400 plus	Roche, Basel
DNA-free™ Kit DNase Treatment & Removal	Thermo Fisher Scientific, Hamburg
Freezer G3013 comfort	Liebherr, Biberach an der Riss
Freezer MDF U53V Ultra low	Sanyo, Munich
gentleMACS Octo Dissociator	Miltenyi Biotec, Bergisch Gladbach
HandyStep® electronic repeating pipette	BRAND GmbH, Wertheim
Incubator Hercell 240	Thermo Fisher Scientific, Waltham
Magnetic Stirrer IKAMAG® RCT	Janke und Kunkel, Staufen
Microscope CK40	Olympus, Hamburg
Mini Cell XCell Sure Lock	Invitrogen, Darmstadt
MyCyclerTM Thermal Cycler	Biorad, Hercules
NanoDrop ND-100	Peqlab, Erlangen
Neubauer Improved	Chamber Roth, Karlsruhe
Pipetboy Integra	INTEGRA Biosciences, Fernwald
Pipettes Eppendorf Research® Plus	Eppendorf, Hamburg
PowerPac HC Power Supply	Biorad, Hercules
QuantStudio 7 Flex	Thermo Fisher Scientific, Hamburg
Scale ATILON ATL-423-I milligram lab balance	Acculab Sartorius group, Göttingen
Scale TE124S analytical weight scale	Sartorius, Göttingen
Tecan Infinite® M200	Tecan, Crailsheim
Thermal Cycler C1000	BioRad, Munich
CFX 96 ™ Real-Time PCR Detection System	
Thermoleader Dry Block Heat Bath	Uniequip, Martinsried
TissueLyser II	Qiagen, Hilden
Versadoc™ Imaging System 4000 MP	Biorad, Hercules
Vortex Mixer	Heidolph, Schwabach

2.1.2. Consumables

Table 2-2 Consumables

Consumable	Supplier
Flow cytometer tubes	Sarstedt, Nümbrecht
Hollow needles/canulaes	B. Braun, Melsungen AG, Melsungen
96-well cell culture plates, round ottom	Sarstedt, Nümbrecht
Cell strainer (100µm)	Corning Inc, Corning
Parafilm M ®	Bemis, Wisconsin
PCR tubes	Abgene, ThermoFisher, Hamburg
Petridishes	Greiner Bio-One, Solingen
Pipette tips (10 µL, 200 µL, 1000 µL)	Sarstedt, Nümbrecht
Pipette tips, sterile and RNAse free (10 µL, 20 µL, 200 µL, 1000 µL)	Sarstedt, Nümbrecht
Pipettes (2 mL, 5 mL, 10 mL, 25 mL)	Sarstedt, Nümbrecht
Positive Displacement Tips (500 µL, 2.5 mL, 5 mL 12.5 mL)	BRAND GmbH, Wertheim
Reaction tubes (1.5 mL, 2 mL)	Sarstedt, Nümbrecht
Reaction tubes (15 mL, 50 mL)	Sarstedt, Nümbrecht
Reaction tubes, sterile and RNAse free (1.5 mL, 2 mL)	Sarstedt, Nümbrecht
Sealing Tape, optically clear	Sarstedt, Nümbrecht
Surgical blade	Feather, Osaka, Japan
Syringes	B. Braun, Melsungen AG, Melsungen
Syringe filter (0.22 µm)	TPP, Trasadingen, CH

2.1.3. Reagents and Kits

Table 2-3 Reagents and kits

Reagents and Kits	Supplier
2-Mercaptoethanol	Gibco®, Invitrogen, Darmstadt
4-(2-hydroxyethyl)-1-piperazineethanesulfonic acid (HEPES)	Roth, Karlsruhe
ALT reagents	Roche, Basel
AP reagents	Roche, Basel
AST reagents	Roche, Basel
Bovine serum albumin (BSA)	Serva, Heidelberg
Brefeldin A (BFA)	Sigma-Aldrich, Taufkirchen
Bio-Plex Pro Human Cytokine Kit	Bio-Rad, Abingdon
dNTPs (10 mM)	Invitrogen GmbH; Darmstadt
Ethylenediaminetetraacetic acid (EDTA)	Roth, Karlsruhe
Ethidiumbromid	Roth, Karlsruhe
Fetal calf serum (FCS)	Lonza, Cologne
Ficoll	Biochrom, Berlin
Foxp3 Staining Buffer Set	eBioscience, Frankfurt
Heparin-sodium-25000-ratiopharm ®	Ratiopharm, Ulm
In Situ Cell Death Detection Kit, TMR Red	Roche, Basel
Ionomycin	Sigma-Aldrich, Taufkirchen

Reagents and Kits	Supplier
LEGENDplex™ Mouse Th cytokine Panel (13-plex)	BioLegend, San Diego
LIVE/DEAD Fixable Staining Kits	ThermoFisher Scientific, Waltham
Maxima™ SYBR Green/ROX qPCR Master Mix (2 x)	Fermentas, Thermo Scientific, Hamburg
Monensin	BioLegend, San Diego
NucleoSpin RNA Kit	Machery-Nagel, Duren
Optiprep®	Sigma-Aldrich, Taufkirchen
Paraformaldehyd	Roth, Karlsruhe
PCR Buffer (10 x)	Invitrogen, Darmstadt
Penicillin/streptomycin (100 U/mL)	Gibco®, Invitrogen, Darmstadt
Percoll	GE Healthcare, Glattbrugg/Zürich
Phorbol 12-myristate 13-acetate (PMA)	Sigma-Aldrich, Taufkirchen
rDNAse	Machery & Nagel, Düren
RPMI	Gibco®, Invitrogen, Darmstadt
Streptavidin horseradish peroxidase (HRP)	R&D, Minneapolis
TMB Substrate Reagent Set	BD Opteia, Heidelberg
Tris-Base	Sigma-Aldrich, Taufkirchen
Tris-HCl	Roth, Karlsruhe
Trypan blue	Sigma-Aldrich, Taufkirchen
Tween 20	Roth, Karlsruhe
Verso cDNA Kit	Abgene, Thermo Scientific, Hamburg

2.1.4. Buffers and Solutions

Table 2-4 Buffers and solutions

Buffer or Solution	Recipe
10 x ACK lysis	1.5M NH4Cl 0.1M KHCO3 1 mM EDTA
10 x Phosphate Buffered Saline (PBS)	137.9 mM NaCl 6.5 mM Na_2HPO_4 x 2 H_2O 1.5 mM KH_2PO_4 2.7 mM KCl Ad to 1 L H2O, pH 7.4
4% Paraformaldehyde	8 g Paraformaldehyde 20 mL PBS (10 x) 10 mM NaOH ad 200 ml ddH_2O, pH 7.4
Acetate citrate buffer	0.88 M Sodium 0.24 M Citric Acid 0.20 M Acetic Acid 0.85 M NaOH ad to 1L H2O, pH6.5

Buffer or Solution	Recipe
Ammoniumchloride (NH_4Cl)	19 mM Tris-HCl 140 mM NH_4Cl ad to 1 L H2O, pH 7.2
Chloramine-T solution (10 mL)	127 mg Cholaramine-T 2 mL n-Propanol [50% v/v] ad to 10 mL Acetate citrate buffer
Ehrlich's Reagent (10 mL)	6.6 mL n-Propanol 3.3 mL Perchloric acid 1.5 g Dimethylaminobenz-aldehyde
Fluorescence activated cell sorting buffer (1 L)	980 mL 1x PBS 2 mL NaN3 (0.02 % w/v) 20 mL FCS
Hanks' Balanced Salt Solution (HBSS) (1 L)	403 mg KCl 53 mg Na_2HPO_4 x 7 H_2O 54 mg KH2PO4 353 mg $NaHCO_3$ 191 mg $CaCl_2$ x 2 H_2O 102 mg $MgCl_2$ x 6 H_2O 148 mg $MgSO_4$ x 7 H_2O 8 g NaCl 1.11 g D-Glucose Monohydrate
Ketamine-Xylazin-Heparin (KHX)	8 % Rompun (2%) 12 % Ketamine (100 mg/ mL) 20% Heparin 5000 (IU/ mL) 60% isotonic NaCl
Percoll solution	Percoll 10xPBS 7.5% NaHCO3 HBSS 100 U/mL Heparin
Proteinase K solution	10µg/ mL Proteinase K 10mM TRIS/HCL
Freezing medium	90% FBS 10% DMSO

2.1.5. Software

Table 2-5 Software

Software	Company
Bio-Rad CFX Manager 2.0	Bio-Rad, Hercules
Bio-Rad Data Analysis Software	Bio-Rad, Hercules
BZ-II Analyzer software	Keyence, Neu-Isenburg
BD FACS Diva	BD Biosciences, Heidelberg
FlowJo™10	BD Biosciences, Heidelberg
GraphPad Prism 6	GraphPad Software, San Diego
Image Lab™ 2.0	Bio-Rad, Hercules
MS Office 2013	Microsoft, Redmond
Primer3	Whitehead Institute for Biomedical Research, Cambridge
Quantstudio™ RT-PCR software	Thermo Fisher Scientific, Hamburg
TBASE	Abase, 4D Deutschland GmbH, Eching
Tecan Magellan v6.5	Tecan, Crailsheim
Versa Doc Imaging System 4000 MP	Bio-Rad, Hercules
Windows XP	Microsoft, Redmond

2.1.6. List of antibodies for surface staining

Table 2-6 Antibodies for surface staining - flow cytometry (Anti-mouse)

	Target	***Fluorophore***	***Clone***	***Distributed by***
Anti-mouse	TCR (β chain)	PE-Cy7	H57-597	BioLegend, San Diego
	TCR (γδ chain)	PerCp-Cy5.5	GL3	BioLegend, San Diego
	CD3	BV785	17A2	BioLegend, San Diego
	CD4	BV711	RM4-5	BioLegend, San Diego
	CD8	BV785	53-6.7	BioLegend, San Diego
	Nkp46	APC	29A1.4	BioLegend, San Diego
	CD1d-Tetramer	AF647		NIH Tetramer Core Facility, Atlanta
	CD107a	FITC	1D4B	BioLegend, San Diego
	CD253/TRAIL	PerCp-Cy5.5	N2B2	BioLegend, San Diego
	CD19	BV785	6D5	BioLegend, San Diego
	CD11c	BV605	N418	BioLegend, San Diego
	CD11b	BV711	M1/70	BioLegend, San Diego
	CCR2	PE	475301	R&D systems, Abingdon
	CX3CR1	BV421	SA011F11	BioLegend, San Diego
Anti-human	CD45	BV510	HI30	BioLegend, San Diego
	CD19	APC Cy7	SJ25C1	BioLegend, San Diego
	CD14	PerCp-Cy5.5	HCD14	BioLegend, San Diego
	CD3	PerCp-Cy5.5	SK7	BioLegend, San Diego
	CD56	PE-Dazzle	HCD56	BioLegend, San Diego
	CD16	BV785	3G8	BioLegend, San Diego
	TRAIL	APC	RIK-2	BioLegend, San Diego
	CD4	BV711	RPA-T4	BioLegend, San Diego
	CD8	AF 700	RPA-T8	BioLegend, San Diego

2.1.7. List of antibodies for intracellular staining

Table 2-7 Antibodies for intracellular staining – flow cytometry (anti-mouse)

Target	***Fluorophore***	***Clone***	***Distributed by***
Granzyme B	Pacific Blue	GB11	BioLegend, San Diego
IFNγ	PE-CF594	XMG1.2	BD Pharmigen, San Jose
IFNγ	PE	XMG1.2	BioLegend, San Diego

2.1.8. List of primers

Table 2-8 Oligonucleotide Sequences

Target	***Forward Primer***	***Reverse Primer***	***Reference***
Cxcl9	TGGAGCAGTGTGGAGTTCG	GTAGTGGATCGTGCCTCGG	NM_008599.4
Cxcl10	GCCGTCATTTTCTGCCTCAT	TGCAGCGGACCGTCCTT	NM_021274
Ifnγ	ACAGCAAGGCGAAAAAGGATG	TCTTCCCCACCCCGAATCA	NM_008337.4
Col3a1	GTCCACGAGGTGACAAAGGT	GATGCCCACTTGTTCCATCT	NM_009930
Ccl2	AGCTGTAGTTTTTGTCACCAAG C	GTGCTGAAGACCTTAGGGC A	NM_011333.3

2.1.9. Depletion antibodies

Table 2-9 Depletion antibodies

Depletion antibody	Clone		Distributed by
Anti-IFNγ	R4-6A2	0.5 mg / mouse	BioXCell, Cologne
*InVivo*Mab rat IgG1	HRPN	0.5 mg / mouse	BioXCell, Cologne
anti-Thy1.2	30H12	0.25 mg / mouse	BioXCell, Cologne
*InVivo*Mab rat IgG2b	LTF-2	0.25 mg / mouse	BioXCell, Cologne
anti-asialo GM1-Ab		25 µL / mouse	Wako Chemicals GmbH, Neuss
rabbit serum		25 µL / mouse	Wako Chemicals GmbH, Neuss

2.1.10. Clinical parameters of patients

Table 2-10 Clinical parameters of PSC, PBC and AIH patients.

	healthy control	**PSC**
n	**8**	**9**
Age	30.3 ± 2.4	44.3 ±13.9
Sex (f/ m)	3/5	5 / 4
Platelets (Mrd/ L)	-	257 ± 121.2
Leucocytes (/µL x 1000)	-	6,6 ± 1.6
Albumin (mg/ dL)	-	36.5 ± 4.6
AST (U/ L)	-	35.1 ± 13.7
ALT (U/ L)	-	42,8 ± 17.6
GGT (U/ L)	-	170.3 ± 153.5
AP (U/ L)	-	152.9 ± 65.8
Bilirubin (mg/ dL)	-	0.7 ± 0.3
Creatinine (mg/ dL)	-	0.9 ± 0.36

Cohorts for analysis of serum IFNγ levels. Data show mean values ±SD

Table 2-11 Clinical parameters of PSC patients undergoing liver transplantation and control patients undergoing liver resection due to tumor metastases

	PSC						"controls"					
	1	**2**	**3**	**4**	**5**	**6**	**7**	**8**	**9**	**10**	**11**	**12**
Age	38	61	67	31	40	68	67	68	45	43	53	55
Sex (f/ m)	f	m	m	m	f	m	f	m	m	f	m	m
Platelets (Mrd/ L)	49	136	196	83	109	349	245	162	247	617	201	189
Leucocytes (/µL x 1000)	6.3	9.7	9.9	6.9	4.5	13.0	3.6	7.5	4.6	9.8	10.2	5.9
Albumin (mg/ dl)	13.2	23.9	26.8	27.4	24.6	1.18	40.5	34.5	42.0	29.1	39.9	37.7
AST (U/ L)	143	109	21	134	115	64	48	36	55	42	36	20
ALT (U/ L)	112	90	17	129	29	54	35	< 6	185	44	59	26
GGT (U/ L)	95	592	219	527	448	219	517	181	109	125	60	47
AP (U/ L)	194	642	66	338	286	167	175	149	82	718	83	36
Bilirubin (mg/ dL)	21.5	12	1.6	23.1	4.2	0.7	0.8	0.5	0.3	0.3	0.5	0.8
Creatinine (mg/ dl)	1.2	1.1	0.95	0.72	0.91	0.86	0.8	1.0	1.2	0.8	1.0	1.1
Cholestasis	+	+	+	+	+	+	+	+	-	+	-	-
Diagnoses							CLM	CLM	CLM	LA	FNH	CLM

CLM= colorectal liver metastasis; LA= liver adenoma; FNH = focal nodular hyperplasia

2.2. Methods

2.2.1. Patient samples

Peripheral blood samples were obtained from patients suffering from PSC (n = 9) recruited at the University Medical Center Hamburg-Eppendorf and from healthy donors (n = 8) enrolled in the Hamburger *"Gesundkohorte".* Liver tissue samples were collected from PSC patients (n = 6) undergoing liver transplantation in the Department of Hepatobiliary and Transplant Surgery of the University Medical Center Hamburg-Eppendorf. As controls, liver samples from patients undergoing liver resection due to tumor metastases were used (n = 6-8; Department of General and Visceral Surgery at the Asklepios Clinic Hamburg-Barmbek). The clinical parameters of these patients are depicted in Table 2-10 and 2-11. All patients provided informed written consent according to study protocols approved by the Medical Association (Ärztekammer) Hamburg (PV4898, PV4081, and PV4780).

2.2.2. Mice

Mdr2$^{-/-}$ mice (C57BL/6.129P2-Abcb4^{tm1Bor}) used for the analysis of chronic liver inflammation were kindly provided by Daniel Goldenberg (Goldyne Savad Institute of Gene Therapy, Jerusalem, Israel). *Mdr2*$^{-/-}$ x *Rag1*$^{-/-}$ mice (C57BL/6.129S7-*Rag1*^{tm1Mom}/129P2-Abcb4^{tm1Bor}/J/J) were obtained from Samuel Huber (I. Department of Medicine, UKE, Hamburg, Germany) and *Ifng*$^{-/-}$ mice (C57BL/6.129S7-(Ifnγ)^{tm1Ts}/J) were kindly given by Hans-Willi Mittrücker (Institute of Immunology UKE, Hamburg, Germany). *Mdr2*$^{-/-}$ x *Ifng*$^{-/-}$ mice were generated by crossbreeding homozygous specimens of the single knockouts. Successful knockout was confirmed via PCR analysis. In addition, C57BL/6 mice were used as controls. All mice received human care according to the guidelines of the National Institutes of Health and to the legal requirements in Germany. Mouse experiments were conducted according to German animal protection law and approved by the institutional review board (Behörde für Gesundheit und Verbraucherschutz, Hamburg, Germany). Mice were housed in IVC cages under controlled conditions (22°C, 55 % humidity, and 12-hour day-night rhythm) and fed a standard laboratory chow (LASvendi, Altromin, Germany).

2.2.3. Animal treatment

For the depletion experiments, 10-week old *Mdr2*$^{-/-}$ mice were treated with the respective antibodies (Ab) or isotype controls intraperitoneally. *Mdr2*$^{-/-}$ mice were injected with an

anti-IFNγ Ab/ *InVivo*Mab rat IgG1 (both 0.5 mg/mouse) or anti-Thy1.2 Ab / *InVivo*Mab rat IgG2b (both 0.25 mg/mouse) or anti-asialo GM1-Ab/ rabbit serum (both 25 µL/mouse) twice a week for 2 weeks. Following treatment, the mice were anesthetized by an intravenous injection of (100µL/10g mouse) a ketamine (120 mg/kg) xylazine (16 mg/kg) heparine (8333 I.E./ kg) solution and were sacrificed by cervical dislocation. The organs and the blood were further analyzed.

2.2.4. Assessment of liver enzyme activity

Heart blood was withdrawn from each mouse and was centrifuged for 5 min at maximal speed (20000 x g) at 4°C. The plasma was stored at -20°C until usage. In order to quantify liver injury, plasma enzyme activities of alanine aminotransferase (ALT), alkaline phosphatase (AP), γ-glutamyltransferase (γ-GT) and aspartate transaminase (AST) were measured using a COBAS Integra 400. Beforehand, the plasma samples were diluted 1:5 with ddH_20.

2.2.5. Isolation of non-parenchymal cells from human liver tissue

The liver was cut into small pieces and homogenized using gentleMACS Octo Dissociator. The liver suspension was poured through several different filters with descending filter sizes (300 µm, 200 µm, 100 µm, 70 µm and 40 µm) to get single cell suspensions. In order to dispose of hepatocytes, the liver suspension was centrifuged at 40 x g for 4 min at room temperature (RT) and the supernatant was retrieved carefully. This step was repeated. After another centrifugation step (500 x g for 5 min at RT), the pellet was resuspended in 4.5 mL PBS and added to 2.5 mL Optiprep solution and mixed carefully. On top of the Optiprep suspension 1 mL of PBS was laid and the samples were centrifuged at 400 x g for 20 min at RT without brake. Afterwards, the interphase containing erythrocytes and leukocytes was taken and washed with PBS. Following lysis of the erythrocytes with ACK buffer for 3 min, the reaction was stopped with PBS and the cell number was counted. Finally, the cells were resuspended in freezing medium and stored at -196°C for further use.

2.2.6. Isolation and re-stimulation of murine hepatic non-parenchymal cells

The murine liver tissue was squashed using the backside of the syringe plunger and the liver suspension was passed through a 100 µm filter. After washing with HBSS and centrifugation (500 g for 5 min at RT), the pellet was resuspended in a 10 mL percoll solution and centrifuged (800 x g for 20 min at RT + brake: 7). Following the removal of

the top layer and the supernatant, the pellet was lysed in ACK buffer for 3 min to remove erythrocytes. The reaction was stopped with HBSS. In order to analyze the cytokine production, the non-parenchymal cells (NPCs; 100000 cells/well) were re-stimulated with phorbol-12-myristate-13-acetate (PMA, 50 ng/mL) and ionomycin (1 µg/mL) for 4 h at 37°C in a 96-well round bottom culture dish. The supernatants of the re-stimulated NPCs were collected after centrifugation (500 g for 5 min at RT) and stored at -20°C. For the analysis of intracellular cytokine production, brefeldin A (50 ng/mL) and monensin (1 µg/mL) were added additionally to the re-stimulation medium after 30 min and incubated for additional 4.5 h. Moreover, for some experiments, anti-CD107a-Ab was added to the re-stimulation medium to evaluate the cytotoxicity of CD8+ T cells and NK cells.

2.2.7. Determination of cytokine levels

LEGENDplex

Cytokine levels in the supernatants of re-stimulated murine NPCs were quantified using LEGENDplex™ Mouse Th cytokine Panel (13-plex) according to the manufacturer's instruction. This multiplex system uses the principles of sandwich enzyme-linked immunosobent assay (ELISA) to quantify soluble analytes by flow cytometry. Briefly, 6.25 µL of the supernatants or standard solutions (serial dilution in assay buffer from 0 to 10000 pg/mL) were mixed with 6.25 µL capture beads thoroughly in a V-bottom 96-well-plate and incubated on a shaker overnight at 4°C. The following day, 6.25 µL of the biotinylated detection antibody cocktail was added to the mixture and incubated on a shaker for 2 h at RT. Afterwards, 6.25 µL of streptavidin-PE (SA-PE) was added and incubated for 0.5 h at RT in the dark. Following several washing steps (1000 x g, 5 min), the samples were analyzed with a Canto II. The evaluation of the data was conducted using the LEGENDplex™ software.

Bio-Plex Pro

IFNγ concentrations in plasma samples of PSC patients and healthy controls were measured using a Bio-Plex Pro Human Cytokine Kit according to the manufacturer's instruction. This magnetic bead-based multiplex assay was performed in cooperation with the group of Markus Altfeld (Heinrich-Pette-Institut, Hamburg).

2.2.8. Hematoxylin & Eosin staining

Hematoxylin & eosin staining was performed on paraformaldehyde-fixed liver sections in order to identify histomorphological features. The staining was carried out in cooperation with the department of pathology (UKE) using standard procedures. The scoring of the liver sections was done by a pathologist specialized in liver pathology in a blinded fashion. Liver inflammation was scored according to the modified hepatitis activity index (mHAI score; (56)) and fibrosis was scored as suggested by the METAVIR-working group (57). Images were taken with a BZ-9000 microscope (Keyence, Neu-Isenburg, Germany).

2.2.9. Sirius Red Staining

Sirius Red staining allows the visualization of fibrotic remodeling in liver tissue by staining hepatic collagen. The staining was performed on paraformaldehyde-fixed liver sections. At first, the sections were deparaffinized and rehydrated in xylol (2 x 10 min) and in a series of ethanol with descending concentrations (100 %, 96 %, 80 %, 70 %, and 50 %) for 5 min/each. As a final step, the sections were incubated in ddH_2O for 2 min followed by incubation of the sections in 0.1% Sirius red solution in saturated picric acid for 90 min at RT. Afterwards, liver sections were placed in 0.01 N HCL for 15 s. The dehydration occurred by incubating the sections in a series of ascending ethanol concentrations (50 % for 30 s, 70 % for 1 min/each and 100 % 4 min). Prior to mounting, the slides were washed with xylol twice for 3 min. Quantification of Sirius Red-positive areas was performed with BZ-II Analyzer software.

2.2.10. Hydorxyproline assay

Hepatic hydroxyproline (Hyp) content was quantified in order to determine collagen level in liver tissue and subsequently to analyze liver fibrosis (58). 100 mg of the shock-frozen liver tissue was homogenized in 900 µL ice-cold distilled water with a tissue lyser (2 min, 30 Hz). The proteins were precipitated by adding 125 µL of 50 % trichloroacetic acid. Afterwards, the samples were incubated for 20 min on ice. Following centrifugation (6000 rpm, 10 min, 4 °C), 1000 µL ice cold ethanol (100 %) was added and the pellets were disrupted using a tissue lyser (30 s, 30 Hz). The last step was repeated and after a final centrifugation step (6000 rpm, 10 min, 4 °C), the pellets were dried upside down for 10 min. Thereafter, samples were hydrolyzed in 800 µL HCl (6 N), sonificated and incubated for 18 h at 110 °C. Next day, the samples were cooled to RT and centrifuged (14000 rpm, 10 min, RT). The supernatants were filtered using a 0.22 µm filter.

Meanwhile, the Hyp standard was prepared as a series of dilutions of Hyp working solution starting with 0.5 µg/µL and further diluted with 6 M HCL. The range of the standard was from 0 to 0.5 µg/µL. Finally, 40 µL of the filtered samples or standards were taken and added to 10 µL NaOH (10 M) and 450 µL of Chloramine-T solution and incubated for 30 min at RT. After incubation, 500 µL of Ehrlich's reagent was added to the samples and incubated at 65 °C for 20 min. Following cooling, the samples were measured in a 96-well plate with the microplate reader (Tecan Infinite M200) at an excitation of 560 nm.

2.2.11. TUNEL assay

TUNEL (Terminal deoxynucleotidyl transferase dUTP nick end labeling) is used to identify the 3'-hydroxyl termini in the double-strand DNA breaks generated during apoptosis. The assay was performed according to the manufacturer's protocol. Briefly, paraformaldehyde-fixed liver sections were deparaffinized using xylol and ethanol. The sections were incubated for 4 min in each of the following solutions at RT: xylol I, xylol II, 100 % EtOH, 90 % EtOH, 70 % EtOH, 50 % EtOH and finally, they were rehydrated in ddH_2O. After a washing step with PBS (3 x 2 min), the samples were incubated in 100 µL Proteinase K-solution for 20 min at 37 °C. Following washing steps with PBS (2 x 3 min), the sections were incubated with 50 µL TUNEL reaction mixture for 60 min at 37 °C. After another washing step (3 x 5 min), the samples were stained with DAPI (1 min at RT). Images were taken with a BZ-9000 microscope. Quantification of TMR Red-positive areas was performed with BZ-II Analyzer software and ImageJ.

2.2.12. Quantitative real-time polymerase chain reaction (qRT-PCR) analysis

The quantitative real-time reverse-transcriptase polymerase chain reaction (qRT-PCR) was performed to analyze the expression of target genes involved in IFNγ signaling and fibrosis. Total RNA was isolated from shock-frozen liver tissue using the NucleoSpin RNA Kit according to the manufacturer's instruction. Genomic DNA was digested using the DNA-free™ Kit DNase Treatment & removal. Finally, 1 µg of RNA was transcribed into cDNA using the Verso cDNA Synthesis Kit on a MyCycler thermal cycler. Quantitative RT-PCR was performed using the ABsolute qPCR SYBR Green Mix. The relative mRNA levels were calculated using the ΔΔCT method after normalization to the reference gene *mitochondrial ATP synthase*. Quantification was shown in x-fold changes to the

corresponding control cDNA. Primers were obtained from Metabion (Martinsried, Germany). Sequences of the primers are listed in Table 2-8.

2.2.13. Flow cytometry

Characterization of the NPCs was done by flow cytometry. For the analysis, 1 x 10^6 freshly isolated cells or re-stimulated *ex vivo* cells were incubated with anti-CD16/32 Ab prior to surface staining in order to prevent unspecific binding. Following washing with FACS buffer (500 x g for 5 min at 4°C), the cells were stained with the respective antibody cocktails, which included the viability dyes depending on the panel (Fixable Viability Dye eFluor™ 506 or red-fluorescent reactive dye). Details about the antibodies used for surface staining are summarized in Table 2-7. Cells stained with antibodies detecting macrophages and lymphocytes were washed with PBS and analyzed with a LSR Fortessa™ flow cytometer. For the analysis of cytokine production of T cells, intracellular staining was necessary. Therefore, the cells were fixed and permeabilized using the BD Cytofix/Cytoperm™ Kit according to the manufacturer's instructions. The antibodies for intracellular staining are listed in Table 2-7. Finally, the cells were washed with permeabilization buffer and analyzed with the LSR Fortessa™ flow cytometer.

2.2.14. Gating strategy

The data obtained from the LSR Fortessa™ flow cytometer were analyzed using FlowJo software. The gating strategies applied to identify T-cell populations and NK cells are depicted in Fig. 7. First, leukocytes were identified via their cell size (forward scatter, FSC) and granularity (sideward scatter, SSC). In order to distinguish single cells from cell aggregates, a diagonal gate within the FSC-H and FSC-A plot was used. Following this, the living cells were defined by selecting the cells, which weren't stained by the viability dye. These cells were further separated by their expression of T cell receptor (TCR) β and TCRγδ and from the TCRβ$^+$ population, the CD4$^+$ T cells, the CD8$^+$ T cells and the CD1d-Tetramer$^+$ NKT cells were gated. For the identification of NK cells within the TCRβ$^-$ cell population, the NKp46$^+$ cells were determined.

In Fig. 8, the gating strategy for human NK cells is outlined. Similar to the strategy described above, the first gate targets the leukocytes. The single cells were identified by gating at FSC-H against FSC-A. Afterwards, the living CD19$^-$ cells were gated and within this population the CD45$^+$ hematopoietic cells were identified. The NK cells, which are characterized as CD56$^+$ CD16$^{+/-}$ were finally determined after exclusion of cells stained

for the markers CD3 expressed by T cells, CD14 expressed by macrophages, and CD127 up-regulated by ILC1. Additionally, the TRAIL expression within the NK cell population was depicted in the last plot.

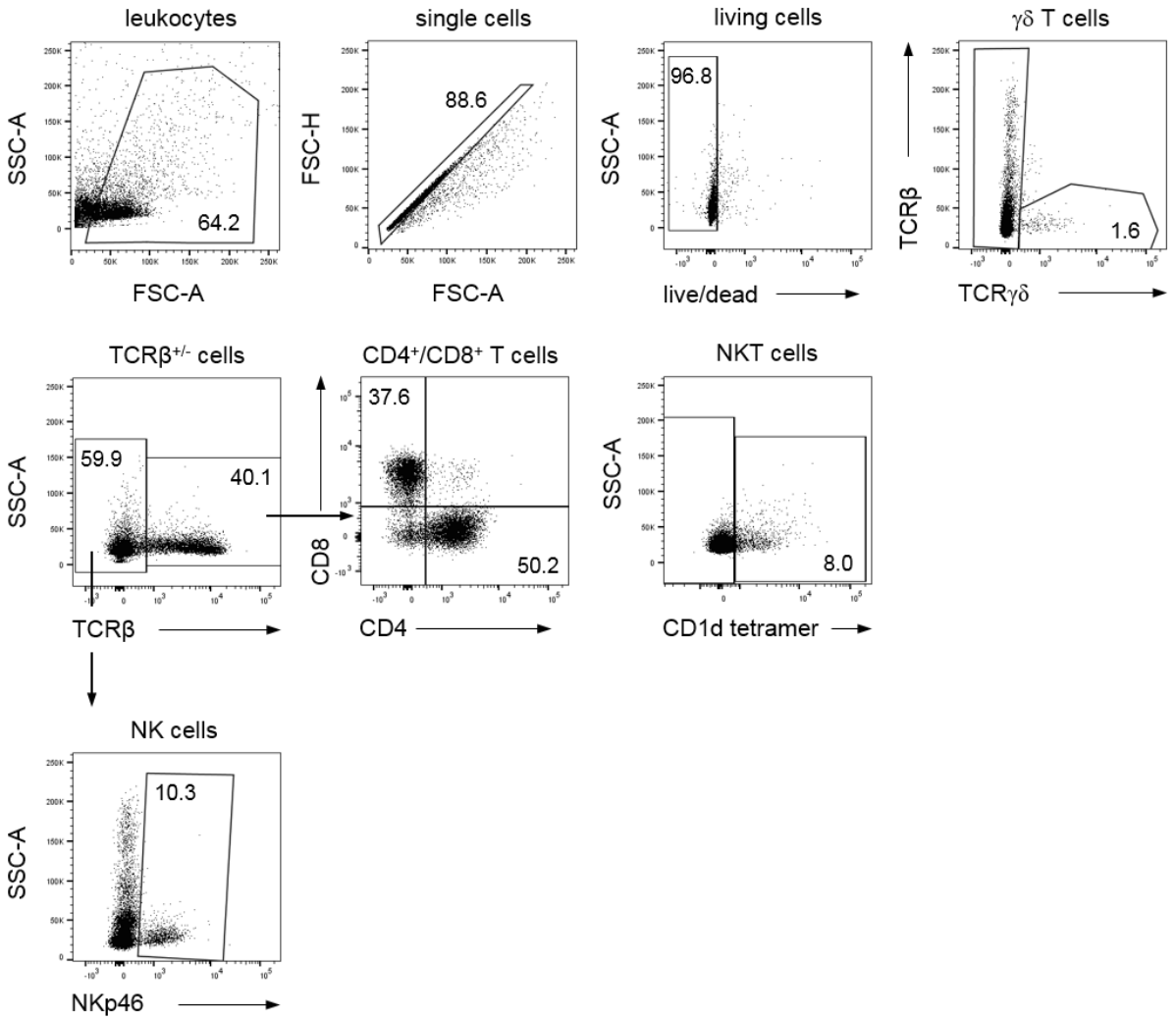

Fig. 7: Gating strategy used for flow cytometry analysis of murine T cells, NKT cells and NK cells. Hepatic lymphocytes from *Mdr2*$^{-/-}$ mice were stained with live/dead dye and antibodies described in Table 2-6. The gating strategy applied to identify TCRβ^{+} CD4^{+} T cells, TCRβ^{+} CD8^{+} T cells, TCRβ^{+} NKT cells and TCRβ^{-} NK cells is shown in the representative dot plots.

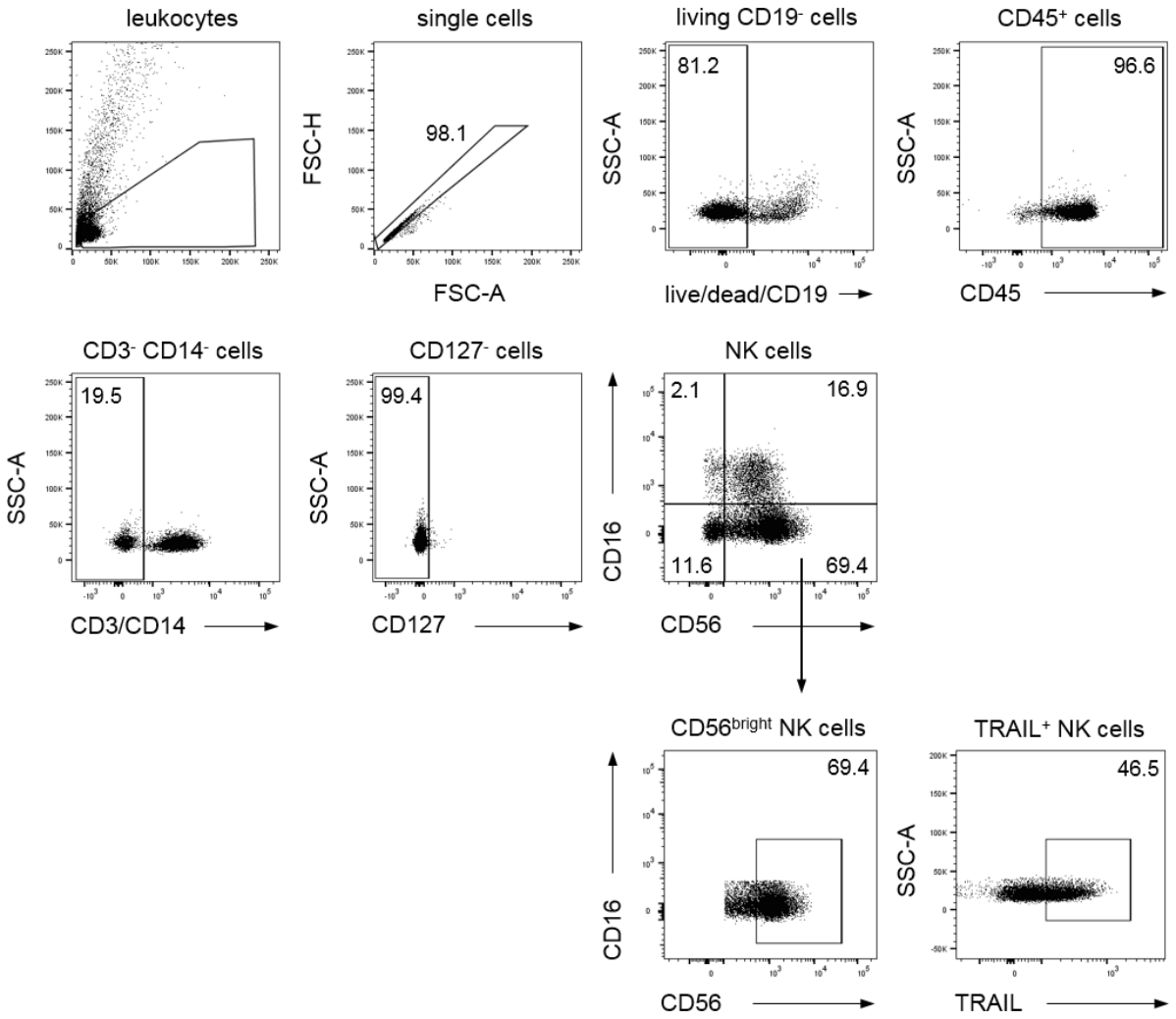

Fig. 8: Gating strategy used in flow cytometry analysis of human NK cells. Human hepatic lymphocytes were stained with live/dead dye and antibodies described in Table 2-6. The gating strategy applied to identify CD19$^-$ CD45$^+$ CD3$^-$ CD14$^-$ CD127$^-$ CD16$^-$ CD56$^+$ NK cells are shown in the representative dot plots.

2.2.15. Statistical Analysis

Statistical analyses were performed using GraphPad Prism 7 software (GraphPad software, San Diego, CA). All data are presented as mean ± SEM. For comparisons between two groups, a non-parametric Mann-Whitney U test and for more than two groups, a one-way ANOVA with Tukey's post-hoc test was used. The ROUT method was used to identify outliers. A p value of less than 0.05 was considered statistically significant with the following ranges *p≤ 0.05, **p≤ 0.01, ***p≤ 0.001, ****p≤ 0.0001.

3. Results

Despite the recognition of PSC as an immune-mediated biliary disease, the underlying mechanisms in the immune pathogenesis are still elusive and under investigation. However, accumulation of IFNγ-expressing Th1 cells around the bile ducts (30,31) and an up-regulation of IFNγ-induced chemokines in the sera of PSC patients (5,6) implicate an involvement of IFNγ in disease progression. The aim of this study was to assess the role of the pleiotropic cytokine IFNγ in the development and progression of PSC. In order to address this question, the following experiments were performed in multidrug resistance protein 2 knockout (*Mdr2*$^{-/-}$) mice (both genders), since they were known to best resemble human PSC.

3.1. *Mdr*2$^{-/-}$ mice developed chronic biliary inflammation and fibrosis

As described in chapter 1.8 the *Mdr2*$^{-/-}$ mice lack the Mdr2 p-glycoprotein leading to a dysfunctional phosphotidylcholine secretion from hepatocytes into the bile canaliculi. As a result, bile acids deploy their hepatoxicity thereby promoting chronic biliary inflammation and fibrosis (50). In order to verify the phenotype, *Mdr*2$^{-/-}$ mice were compared with C57BL/6 WT mice. The mice were analyzed at the age of 12 weeks due to their pronounced development of fibrotic chronic liver phenotype at this time point. Control mice were picked from the same age. Hepatic injury was analyzed by measuring the activities of liver enzymes such as ALT, AST and AP in the plasma. Additionally, since elevated bilirubin levels are associated with increased probability for cholestasis (21), bilirubin was measured in the plasma of *Mdr2*$^{-/-}$ and WT mice. Biliary inflammation was quantified by the mHAI score. Hepatic collagen deposition was additionally determined by measuring the Hyp content, by Sirius red staining and quantification of collagen type III α 1 chain (*Col3a1)* mRNA expression.

Mdr2$^{-/-}$ mice showed elevated plasma levels of ALT (Fig. 9 A), AST (Fig. 9 B) and AP (Fig. 9 C) compared to C57BL/6 WT mice pinpointing tissue damage. Moreover, *Mdr2*$^{-/-}$ mice showed slightly elevated levels of bilirubin unlike WT mice (Fig. 9 D). The mHAI score was significantly increased (Fig. 9 E) in *Mdr2*$^{-/-}$ mice compared to the control mice. The amount of Hyp (Fig. 9 F) as well as the hepatic mRNA expression of *Col3a1* (Fig. 9 G) and percentage of Sirius red positive area (Fig. 9 H) were analyzed in order to determine levels of fibrosis. All three markers were significantly enhanced in *Mdr2*$^{-/-}$ mice in comparison

to WT mice. Consequently, the development of chronic liver inflammation and fibrosis was confirmed in 12-week-old *Mdr2*$^{-/-}$ mice.

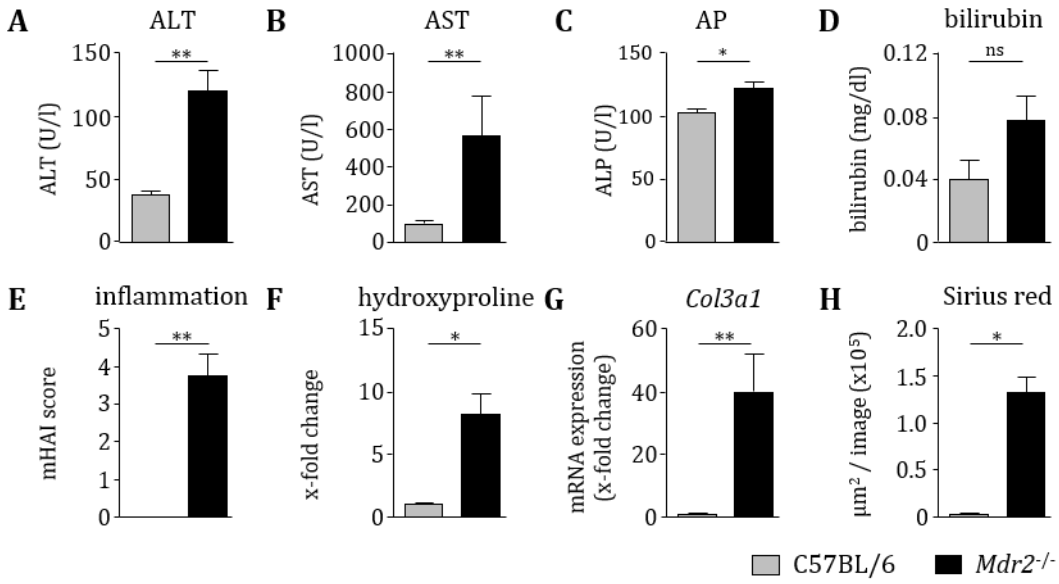

Fig. 9: *Mdr2*$^{-/-}$ mice developed chronic biliary inflammation and fibrosis at an age of 12 weeks. Levels of **(A)** ALT, **(B)** AST, **(C)** AP and **(D)** bilirubin were measured in the plasma of *Mdr2*$^{-/-}$ mice and WT mice. **(E)** The mHAI score was determined by a liver pathologist. **(F)** The hepatic relative Hyp content as well as **(G)** the hepatic mRNA expression of *Col3a1*, determined by qRT-PCR, and **(H)** Sirius red staining, quantified in liver sections, were determined to evaluate liver fibrosis. Data: mean values ± SEM, n = 4-9 (mice), ns: not significant, *p ≤ 0.05, ** p ≤ 0.01. Adapted from Ravichandran *et al*., 2019.

3.2. *Mdr2*$^{-/-}$ mice exhibited increased IFNγ production in T cells and NK cells

Since IFNγ was suspected to play a role in the immune pathogenesis of PSC, the first task was to identify immune cell populations which are able to produce this cytokine in the *Mdr2*$^{-/-}$mice.

The major immune cell populations known to produce IFNγ are T cells and NK cells (3). Therefore, the production of IFNγ by hepatic lymphocyte populations was analyzed in WT and *Mdr2*$^{-/-}$ mice via flow cytometry. As depicted in Fig.10 A, IFNγ was produced by hepatic CD4^{+} T cells, CD8^{+} T cells, NKT cells, γδ T cells and NK cells of WT mice. In *Mdr2*$^{-/-}$ mice, the same immune cell populations were able to produce IFNγ, however, the number of IFNγ-producing lymphocytes was increased (Fig. 10 B). Especially, CD8^{+} T cells and NKT cells were the main IFNγ producers in *Mdr2*$^{-/-}$ mice compared to WT mice. In addition to that, the hepatic mRNA expression of the chemokines *Cxcl9* and *Cxcl10*, which are induced by IFNγ, were up-regulated in *Mdr2*$^{-/-}$ mice (Fig. 10 C). In order to verify the association of IFNγ with PSC, we analyzed IFNγ levels in the sera of PSC patients and

healthy controls. PSC patients displayed elevated levels of IFNγ compared to the healthy controls (Fig. 10 D).

In summary, in comparison to WT mice *Mdr2*$^{-/-}$ mice displayed enhanced production of IFNγ by CD8^{+} T cells and NKT cells and expression of IFNγ-induced chemokines. Up-regulated IFNγ levels were further shown in sera of PSC patients, further supporting investigation of its role in the immune pathogenesis of PSC.

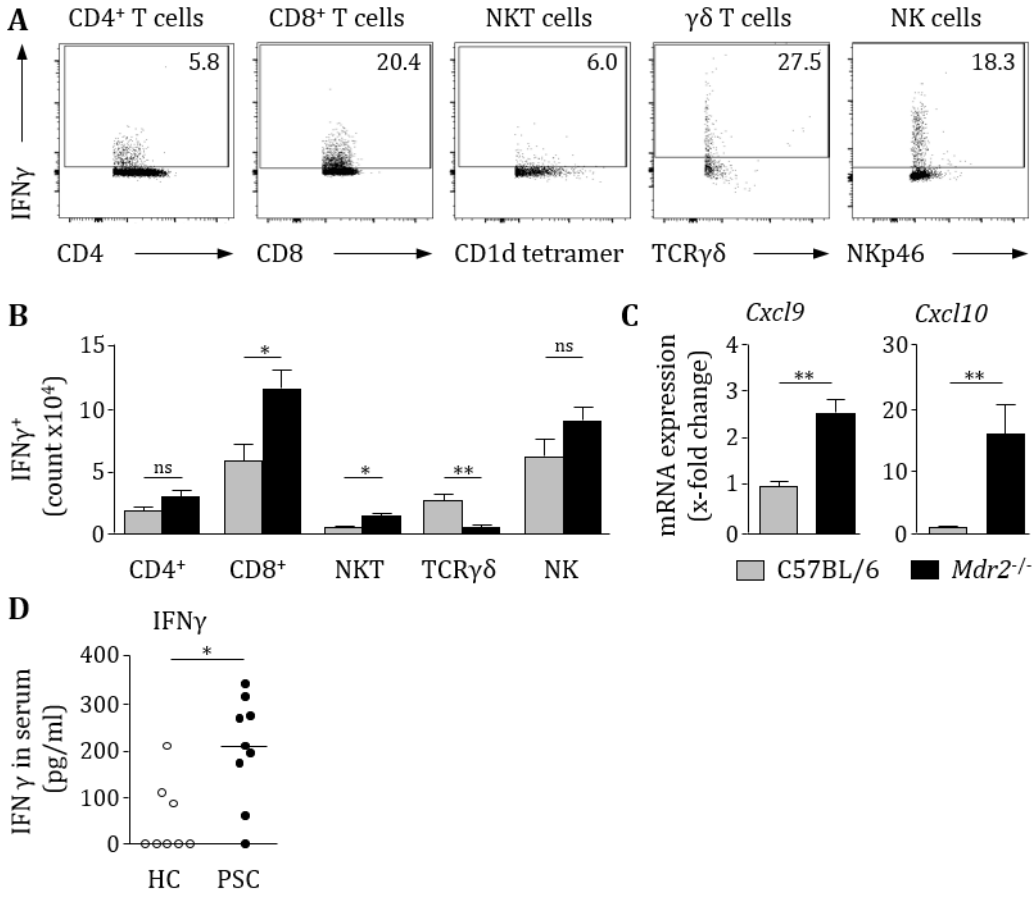

Fig. 10: Increased IFNγ production in *Mdr2*$^{-/-}$ mice and PSC patients. (A) IFNγ–producing immune cells from WT mice were re-stimulated with PMA/ionomycin and shown in representative dot plots. **(B)** Numbers of IFNγ-producing cells from *Mdr2*$^{-/-}$ mice and C57BL/6 WT mice were shown. **(C)** The hepatic mRNA expression of IFNγ-induced chemokines *Cxcl9* and *Cxcl10* were determined by qRT-PCR. **(D)** The IFNγ levels in the serum of PSC patients (n = 9) and healthy controls (HC; n = 8) were measured using Bio-Plex Pro Human Cytokine Kit. Data: mean values ± SEM, n = 5 (mice), ns: not significant, *p ≤ 0.05, ** p ≤ 0.01. Adapted from Ravichandran *et al.*, 2019.

3.3. Depletion of CD90.2$^+$ cells in *Mdr2*$^{-/-}$ mice reduced tissue damage, but not fibrosis

The finding of CD8$^+$ T cells as the major IFNγ source in the *Mdr2*$^{-/-}$ mice and the increased expression of the chemokines *Cxcl9* and *Cxcl10* attracting immune cells to the site of injury suggested an analysis of hepatic accumulation of immune cells by flow cytometry. As shown in Fig. 11 A, numbers of TCRβ$^+$ T cells, CD4$^+$ T cells, CD8$^+$ T cells, NKT cells and NK cells were significantly increased in livers of *Mdr2*$^{-/-}$ mice compared to WT control mice.

Since T cells and NK cells were not only identified to produce IFNγ, but were also increased in frequency in the *Mdr2*$^{-/-}$ mice (Fig. 11 A), the aim was to investigate the contribution of the entirety of these IFNγ-producing cells to PSC pathophysiology by *in vivo* depletion of these cells in *Mdr2*$^{-/-}$ mice.

The depletion of T cells was executed by using an Ab targeting CD90.2 (anti-Thy1.2 Ab), a glycosylphosphatidylinositol (GPI)-linked membrane molecule, expressed by most lymphocytes, especially mouse thymocytes and mature T cells (59,60). Treatment of *Mdr2*$^{-/-}$ mice with an anti-Thy1.2 Ab twice a week for two weeks strongly reduced the number of hepatic CD4$^+$ T cells, CD8$^+$ T cells, and NKT cells (Fig. 11 B).

However, γδ T cells, which produce less IFNγ in the *Mdr2*$^{-/-}$ (Fig. 10 B) mice compared to control mice and represent only a small fraction of liver T cells (Fig, 11 B), were not affected by the anti-Thy1.2 Ab. In contrast to that, the count of NK cells was significantly reduced in anti-Thy1.2-treated *Mdr2*$^{-/-}$ mice, nevertheless, the extent of the reduction was not as striking as for T cells. While IFNγ production by NK cells was not altered following T cell depletion, the cytotoxicity of this cell population was reduced as shown by reduced expression of CD107a, a degranulation marker (Fig. 11 C).

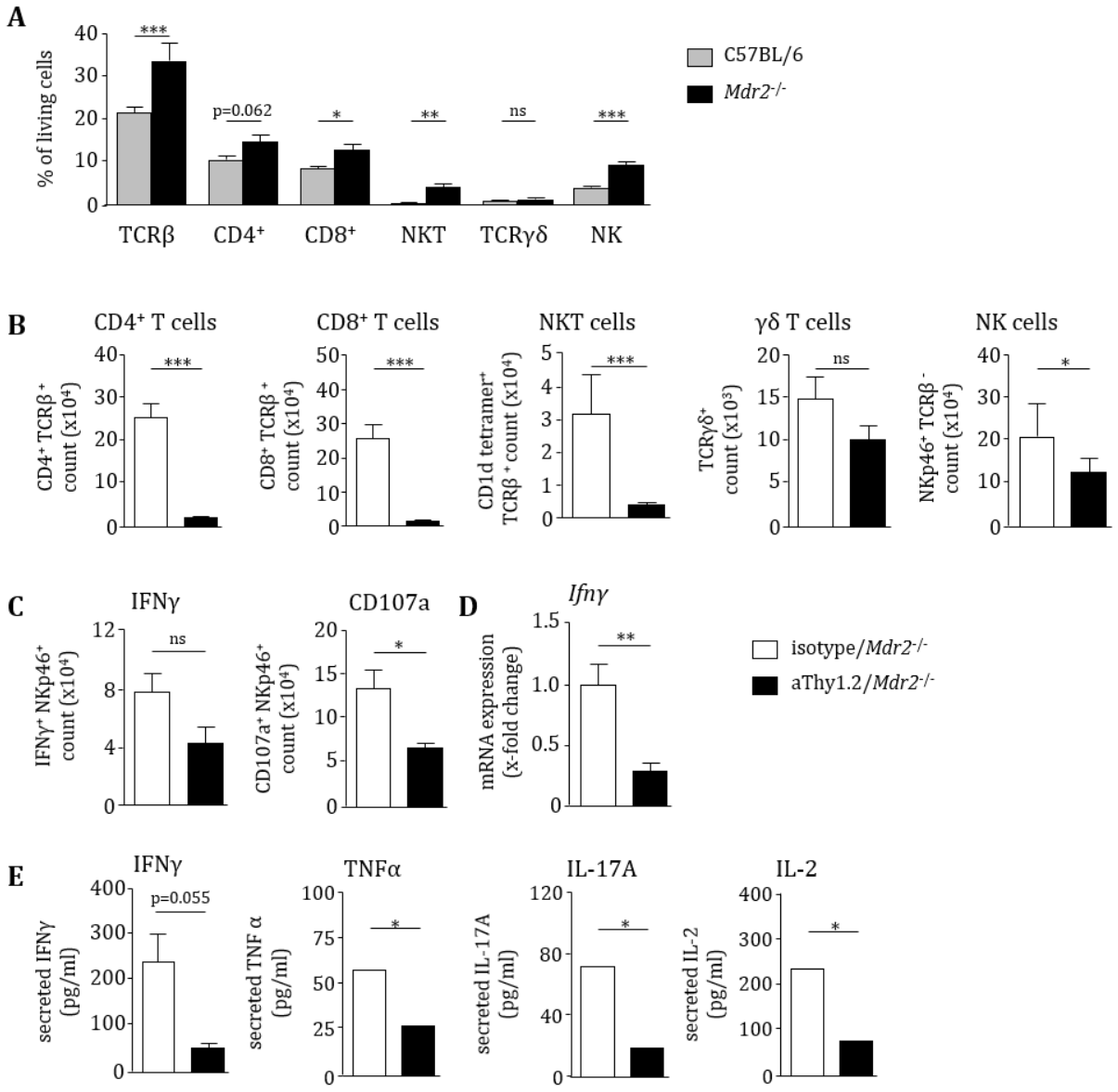

Fig. 11: Application of anti-CD90.2⁺ Ab resulted in T cell depletion and in a reduced production of pro-inflammatory cytokines. (A) Frequencies of hepatic T cells and NK cells were analyzed by flow cytometry in 12-week old *Mdr2*$^{-/-}$ mice. **(B)** 10-week old *Mdr2*$^{-/-}$ mice were treated with anti-Thy1.2 Ab or the isotype control twice a week for 2 weeks. The count of CD90.2⁺ cells were analyzed by flow cytometry. **(C)** Number of IFNγ⁺ and CD107a⁺ NK cells were determined by flow cytometry after re-stimulation with PMA/ionomycin. Anti-CD107a Ab was added to the medium for staining. **(D)** The hepatic mRNA expression of *Ifnγ* was determined in the anti-Thy1.2- and Isotype-treated mice by qRT-PCR. **(E)** Pro-inflammatory cytokines were measured in the supernatant of re-stimulated NPCs using LEGENDplex. Data: mean values ± SEM, n = 5-8 (mice), ns: not significant, *p ≤ 0.05, ** p ≤ 0.01. Adapted from Ravichandran *et al*., 2019.

Following analysis of the count of hepatic lymphocytes after anti-Thy1.2 Ab application, the hepatic expression of *Ifnγ* was quantified in order to define the impact of T cell depletion on cytokine production and its effects on the pathogenesis of PSC. Compared to isotype-treated group, the anti-Thy1.2 Ab-treated group showed significantly reduced IFNγ gene expression (Fig. 11 D). Furthermore, following *ex vivo* re-stimulation of residual liver leucocytes, IFNγ secretion as well as the amount of secreted pro-inflammatory

cytokines such as TNFα and IL-17A were analyzed by LEGENDplex (Fig. 11 E). In comparison to the control animals, anti-Thy1.2 Ab treated mice have significantly diminished levels of the pro-inflammatory cytokines.

The depletion of T cells using anti-Thy1.2 Ab in the *Mdr2*$^{-/-}$ mice resulted in reduced plasma ALT levels (Fig. 12 A). Also, liver inflammation, determined by the mHAI score, tended to be reduced in the anti-Thy1.2 Ab treated group (Fig. 12 B). In contrast to hepatic tissue damage, no effect on fibrogenesis was determined in *Mdr2*$^{-/-}$ mice after anti-Thy1.2 Ab treatment, since no changes in the relative Hyp content, hepatic *Col3a1* mRNA expression and percentage of Sirius Red stained areas were observed in comparison to isotype-treated control mice (Fig. 12 C-E).

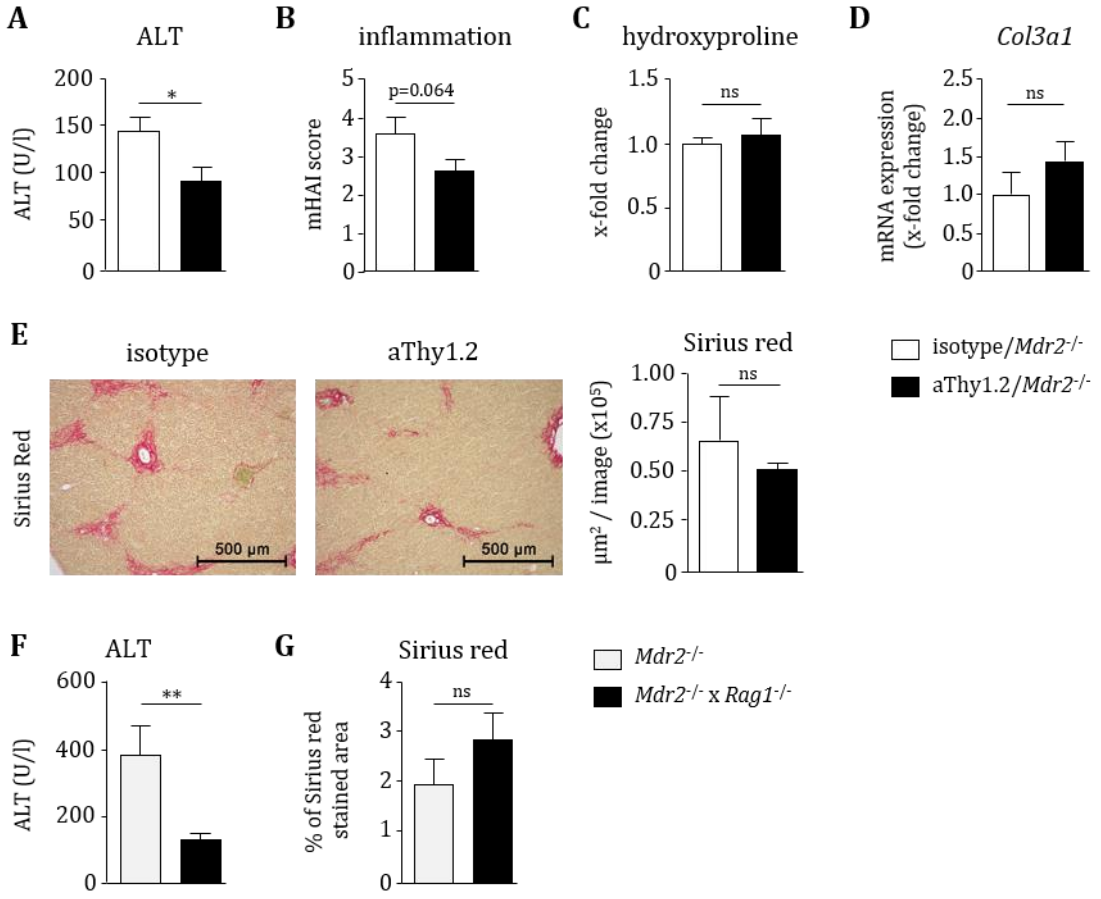

Fig. 12: Depletion of CD90.2⁺ cells reduced liver injury in *Mdr2*$^{-/-}$ mice without having an effect on development of fibrosis. 10-week-old *Mdr2*$^{-/-}$ mice were treated with anti-Thy1.2 Ab or the respective isotype control twice a week for 2 weeks. **(A)** Plasma ALT levels from anti-Thy1.2 or isotype-treated *Mdr2*$^{-/-}$ mice were measured. **(B)** Liver inflammation was calculated using mHAI score. **(C)** The relative Hyp content in the livers of anti-Thy1.2- or isotype-treated mice was determined. **(D)** The hepatic mRNA expression of *Col3a1* was determined by qRT-PCR. **(E)** Sirius Red staining was analyzed by scoring the H&E stained liver section of the treated mice. **(F)** ALT levels were measured in the plasma of the *Mdr2*$^{-/-}$ x *Rag1*$^{-/-}$ mice and *Mdr2*$^{-/-}$ mice. **(G)** Sirius Red staining was quantified in liver slices from *Mdr2*$^{-/-}$ mice and *Mdr2*$^{-/-}$ x *Rag1*$^{-/-}$ mice. Data: mean values ± SEM, n = 5-8 (mice), ns: not significant, *p ≤ 0.05, ** p ≤ 0.01. Adapted

from Ravichandran *et al.*, 2019

Similar results were obtained from *Mdr2*$^{-/-}$ x *Rag1*$^{-/-}$ mice, which lack B and T cells. In regard of tissue damage, the *Mdr2*$^{-/-}$ x *Rag1*$^{-/-}$ mice had reduced ALT levels compared to *Mdr2*$^{-/-}$ mice (Fig. 12 F), confirming the results after T-cell depletion with anti-Thy1.2 Ab. Sirius red staining analysis revealed no alteration in fibrosis between the *Mdr2*$^{-/-}$ and *Mdr2*$^{-/-}$ x *Rag1*$^{-/-}$ mice (Fig. 12 G). Taken together, depletion of T cells was associated with reduced expression of pro-inflammatory cytokines and reduced tissue damage in *Mdr2*$^{-/-}$ mice, while fibrosis was unchanged.

3.4. PSC patients have increased frequencies of hepatic cytotoxic NK cells

The increased frequencies of NK cells and CD8$^+$ T cells in *Mdr2*$^{-/-}$ mice suggested a role of these immune cells in the pathology of sclerosing cholangitis in mice. Hence, in order to explore the immune cell composition in PSC patients, liver samples of explant livers from PSC patients and controls were analyzed by flow cytometry. The control liver samples were obtained from patients undergoing liver resection due to tumor metastases (Table 2-11).

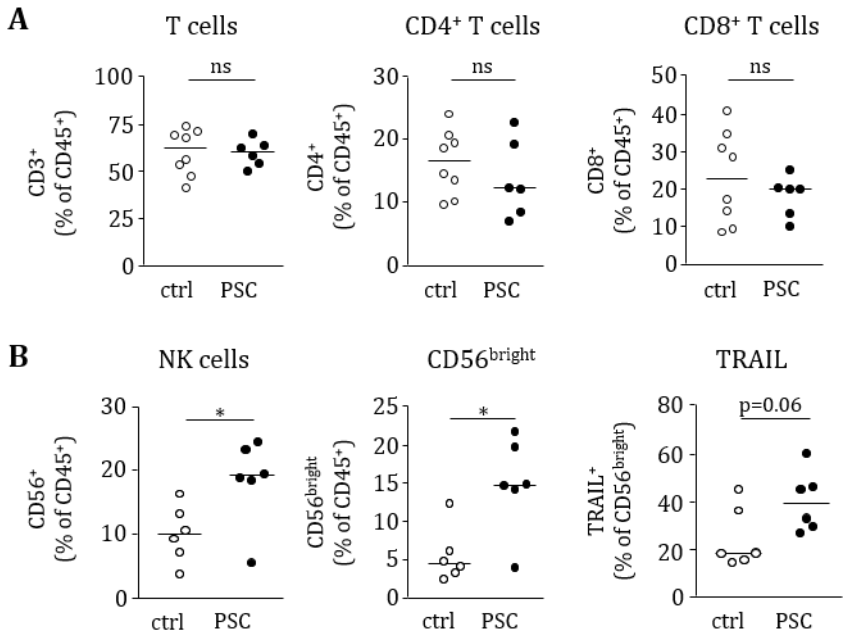

Fig. 13: Frequencies of cytotoxic CD56^{bright} NK cells were increased in PSC patients. (A) Frequencies of hepatic T cells from PSC patients and control patients were analyzed by flow cytometry. **(B)** Frequencies of hepatic NK cells from PSC patients and control patients and their expression of TRAIL were analyzed by flow cytometry. Data: mean values ± SEM, n = 6-8 human samples, ns: not significant, *p ≤ 0.05, ** p ≤ 0.01. Adapted from Ravichandran *et al.*, 2019. ctrl - control

Regarding the T-cell compartment, no differences between the PSC patients (n=6) and the control group (n=6-8) were found. Frequencies of CD3⁺ T cells, CD4⁺ T cells and CD8⁺ T cells were not significantly altered (Fig. 13 A). However, the frequency of CD56⁺ NK cells was elevated in PSC patients compared to the control group. Part of the CD56⁺ NK cells were also even identified to be CD56^{bright} cells, which are known to have properties of tissue residency (61). In addition, these CD56^{bright} cells produced increased levels of TRAIL, a pro-apoptotic molecule, which is capable of interacting with the TNF receptor family on target cells and inducing apoptosis (Fig. 13 B).

3.5. Depletion of NK cells reduced cytotoxicity of CD8⁺ T cells and exerted an anti-fibrotic effect

Due to the enhanced frequency of CD56⁺ NK cells in the liver samples of PSC patients, depletion of NK cells was carried out in order to analyze the potential involvement of NK cells in disease progression. The depletion was performed using Nkp46-specific anti-asialo GM1 Ab and the corresponding control serum in the *Mdr2*$^{-/-}$ mice. Experiments were started at the age of 10 weeks and after two weeks of treatment (2x/week) the mice were sacrificed and analyzed.

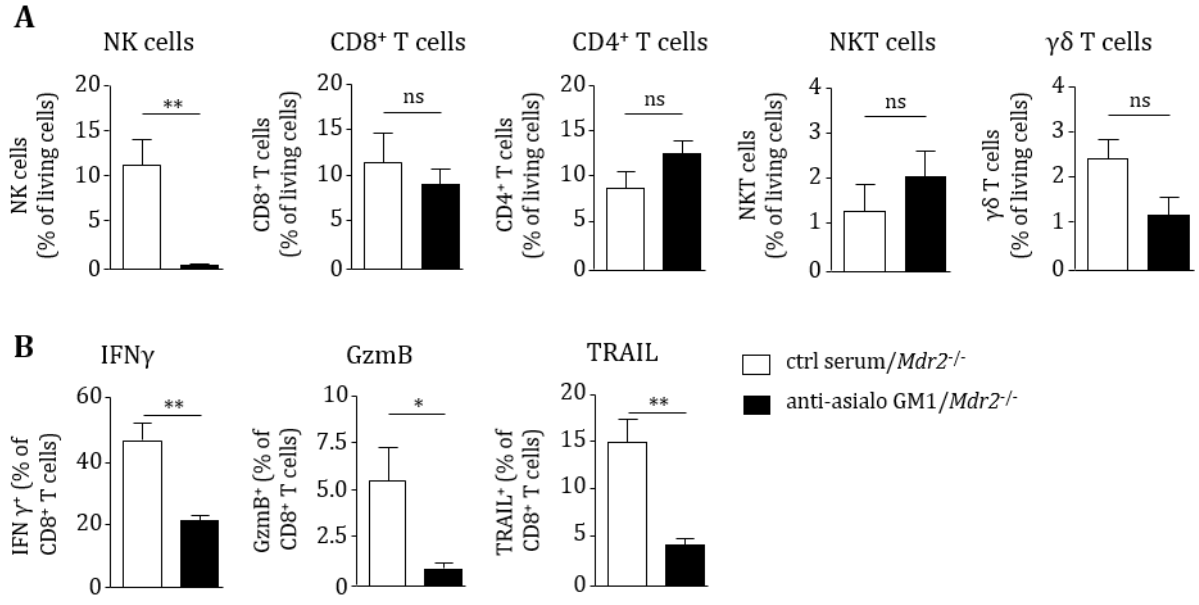

Fig. 14: Depletion of NK cells in *Mdr2*$^{-/-}$ mice reduced the cytotoxicity of CD8⁺ T cells. (A) 10-week-old *Mdr2*$^{-/-}$ mice were treated twice a week over a period of 14 days with anti-asialo GM1 Ab or control serum. Frequencies of T cells, NKT cells, and NK cells after anti-asialo GM1/serum treatment were analyzed by flow cytometry. **(B)** Frequencies of CD8⁺ T cells producing IFNγ, GzmB and TRAIL were analyzed by flow cytometry after NK cell depletion. Data: mean values ± SEM, n = 5 (mice), ns: not significant, *p ≤ 0.05, ** p ≤ 0.01. Adapted from Ravichandran *et al*., 2019.

As evident from Fig. 14 A, application of anti-asialo GM1 Ab led to reduced frequency of NK cells in the *Mdr2*$^{-/-}$ mice. Frequencies of other immune cell populations like CD8^{+} T cells, CD4^{+} T cells, NKT cells and γδ T cells were not affected (Fig. 14 A). However, percentages of IFNγ^{+}, GzmB^{+} and TRAIL^{+} CD8^{+} T cells were reduced in the anti-GM1 Ab treated group compared to the serum-treated control group (Fig. 14 B).

Liver tissue damage determined by the measurement of plasma ALT levels showed no difference between the control and anti-GM1 Ab treated mice (Fig. 15 A). Moreover, the mHAI score, pinpointing liver inflammation, showed no difference between both groups (Fig. 15 B). However, fibrosis was reduced in the anti-asialo GM1 Ab treated *Mdr2*$^{-/-}$ mice in comparison to the control mice. According to the relative Hyp content, the hepatic mRNA expression of *Col3a1* and the percentage of Sirius red stained area (Fig. 15 C-E), fibrosis in the anti-asialo GM1-Ab treated mice was reduced.

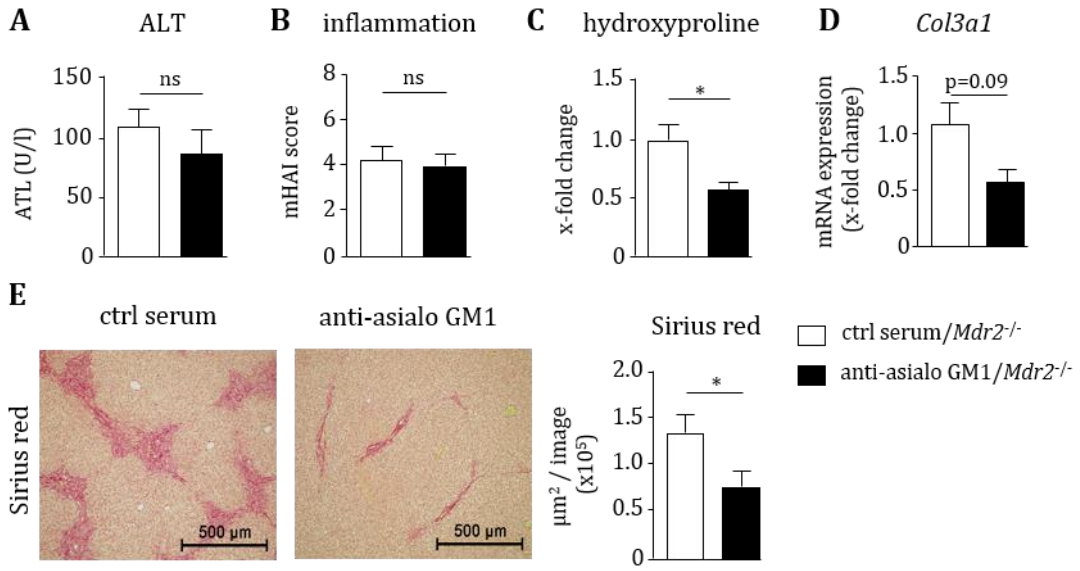

Fig. 15: Depletion of NK cells with anti-asialo GM1 Ab in *Mdr2*$^{-/-}$ mice exerted an anti-fibrotic effect. 10- week old *Mdr2*$^{-/-}$ mice were treated twice a week over a period of 14 days with anti-asialo GM1 Ab or control serum. **(A)** Plasma ALT levels were measured from anti-asialo GM1 Ab- or serum-treated mice. **(B)** The mHAI score was determined by scoring of the H&E stained liver section by a liver pathologist. **(C)** Hyp was quantified in the liver tissue to measure the collagen content. **(D)** The hepatic mRNA expression of *Col3a1* was analyzed by qRT-PCR. **(E)** Sirius Red positive area was quantified in liver slices. Data: mean values ± SEM, n = 5 (mice), ns: not significant, *p ≤ 0.05, ** p ≤ 0.01. Adapted from Ravichandran *et al.*, 2019.

In conclusion, depletion of NK cells in *Mdr2*$^{-/-}$ mice leads to reduced cytotoxicity of CD8^{+} T cells and diminished fibrosis.

3.6. Ablation of IFNγ lead to reduced cytotoxicity of CD8⁺ T cells and NK cells and exerted an anti-fibrotic effect

Depletion of T cells or NK cells using anti-Thy1.2 Ab or anti-asialo GM1 Ab resulted in reduced IFNγ production and in reduced hepatic gene expression of IFNγ-induced chemokines *Cxcl9* and *Cxcl10*. Apart from that, the functional impact of IFNγ on chronic liver inflammation still remained elusive. In order to address this question, *Mdr2*$^{-/-}$ x *IFNg*$^{-/-}$ mice were generated and analyzed in comparison to the *Mdr2*$^{-/-}$ mice and the WT mice at the age of 12 weeks.

As expected, in the *Mdr2*$^{-/-}$ x *IFNg*$^{-/-}$ mice the hepatic immune cell populations CD4⁺ T cells, CD8⁺ T cells, NKT cells, TCR γδ⁺ T cells and NK cells showed no IFNγ production after re-stimulation with PMA/ionomycin (Fig. 16 A). The hepatic gene expression of the chemokines *Cxcl9* and *Cxcl10* was significantly down-regulated in *Mdr2*$^{-/-}$ x *IFNg*$^{-/-}$ mice compared to *Mdr2*$^{-/-}$ mice (Fig. 16 B). Additionally, the frequencies of CD4⁺ T cells, CD8⁺ T cells, NKT cells, γδ T cells and NK cells were reduced in the *Mdr2*$^{-/-}$ x *IFNg*$^{-/-}$ mice in comparison to *Mdr2*$^{-/-}$ mice (Fig. 16 C). In summary, the absence of IFNγ prevented the secretion of IFNγ-induced chemokines and significantly reduced the frequencies of all analyzed lymphocytes in the liver.

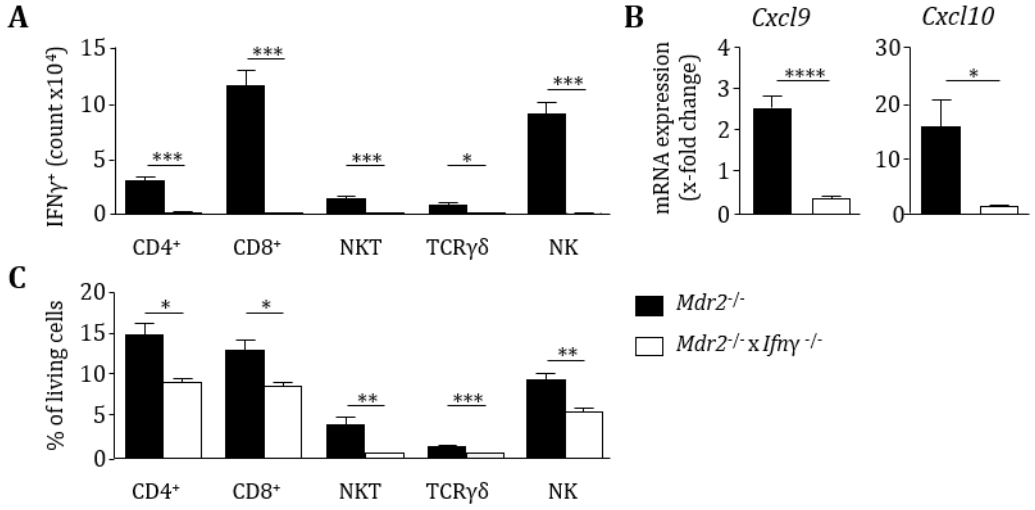

Fig. 16: Reduced frequencies of IFNγ-producing immune cells in the *Mdr2*$^{-/-}$ x *IFNg*$^{-/-}$ mice. (A) In *Mdr2*$^{-/-}$ mice and *Mdr2*$^{-/-}$ x *IFNg*$^{-/-}$ mice, the number of IFNγ-producing immune cells were analyzed by flow cytometry. **(B)** The hepatic mRNA expression of the IFNγ-induced chemokines *Cxcl9* and *Cxcl10* were determined by qRT-PCR. **(C)** The frequencies of T cells, NKT cells and NK cells were obtained by flow cytometry. Data: mean values ± SEM, n = 5 (mice), ns: not significant, *p ≤ 0.05, ** p ≤ 0.01. Adapted from Ravichandran *et al*., 2019

In regard of cytotoxicity, the question emerges whether IFNγ has an impact on the extent of cytotoxicity. For instance, depletion of CD90.2$^+$ cells and NK cells in *Mdr2$^{-/-}$* mice resulted in reduced production of IFNγ and compromised cytotoxicity of NK cells and CD8$^+$ T cells. Furthermore, PSC patients, who have elevated levels of IFNγ in the sera (Fig.10 D), additionally showed an increased expression of TRAIL by CD56^{bright} NK cells. The interaction between IFNγ and cytotoxicity was therefore analyzed in the following three genotypes: WT mice, *Mdr2$^{-/-}$* mice and *Mdr2$^{-/-}$* x *IFNg$^{-/-}$* mice.

In comparison to WT mice, which serve as healthy controls, *Mdr2$^{-/-}$* mice depicted elevated frequencies of GzmB$^+$ and TRAIL$^+$ NK cells and CD8$^+$ T cells. Up-regulation of these markers indicate increased cytotoxic capacities of these cells in chronic liver inflammation. In absence of IFNγ on the other hand, the percentage of NK cells and CD8$^+$ T cells expressing GzmB and TRAIL were diminished, reaching the levels of healthy control mice (Fig. 17). Thus, absence of IFNγ leads to reduced cytotoxicity of NK cells and CD8$^+$ T cells.

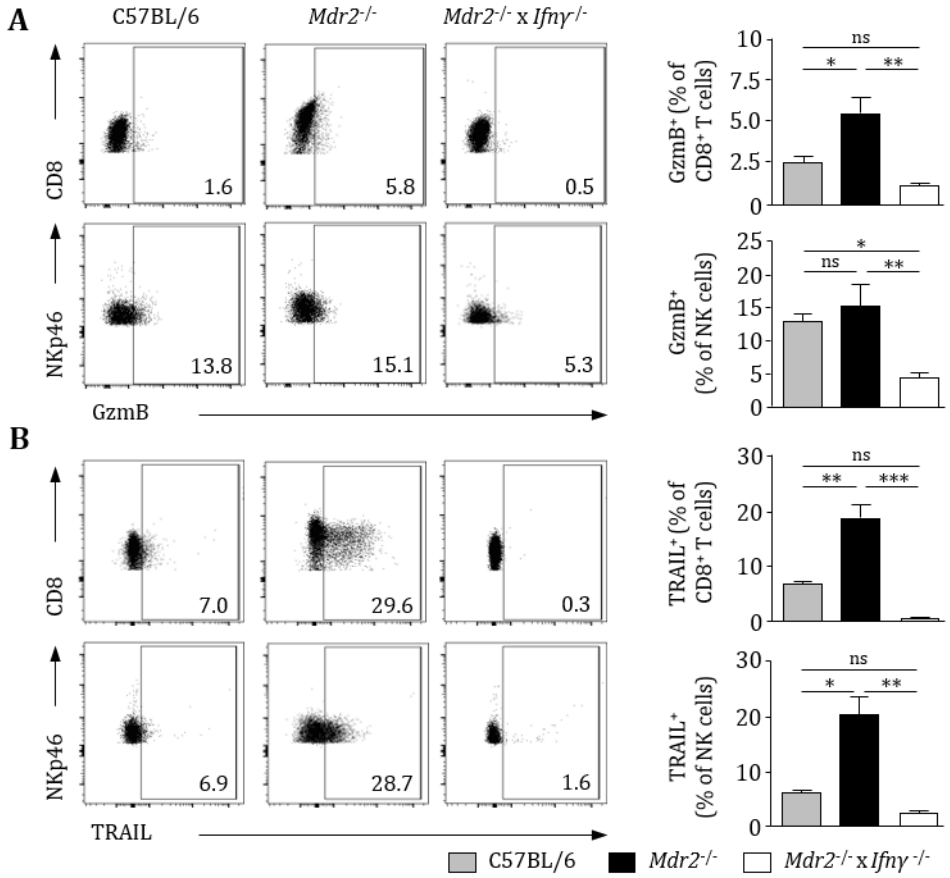

Fig. 17: Ablation of IFNγ led to reduced cytotoxicity of CD8$^+$ T cells and NK cells. (A) The expression of GzmB in CD8$^+$ T cells and NKp46$^+$ NK cells was depicted in representative dot plots for the different genotypes: C57BL/6 WT mice, *Mdr2$^{-/-}$* mice and *Mdr2$^{-/-}$* x *IFNg$^{-/-}$* mice. The quantitative analysis of the flow

cytometry data was shown in diagrams next to the plots. **(B)** The expression of TRAIL in $CD8^+$ T cells and $NKp46^+$ NK cells was shown in representative dot plots for the different genotypes. The quantitative analysis of the flow cytometry data was shown in diagrams next to the plots. Data: mean values ± SEM, n = 5 (mice), ns: not significant, *p ≤ 0.05, ** p ≤ 0.01. Adapted from Ravichandran *et al*., 2019.

Subsequently, it was analyzed whether the elevated cytotoxicity of $CD8^+$ T cells and NK cells in *Mdr2*$^{-/-}$ mice lead to enhanced cell death in the inflamed liver tissue. In addition, the involvement of IFNγ in this process was also explored since ablation of IFNγ already reduced cytotoxicity of these cells and might therefore have an influence on the induction of apoptosis. In order to analyze cell death in *Mdr2*$^{-/-}$ *and Mdr2*$^{-/-}$ x *IFNg*$^{-/-}$ mice, TUNEL assay was performed.

As apparent from Fig. 18, in the *Mdr2*$^{-/-}$ mice around 10% of the stained area was $TUNEL^+$ pinpointing increased accumulation of apoptotic cells in chronic liver inflammation. But in absence of IFNγ as in *Mdr2*$^{-/-}$ x *IFNg*$^{-/-}$ mice cell death was enormously reduced, almost absent. Taken together, absence of IFNγ reduces cell death in chronic liver inflammation.

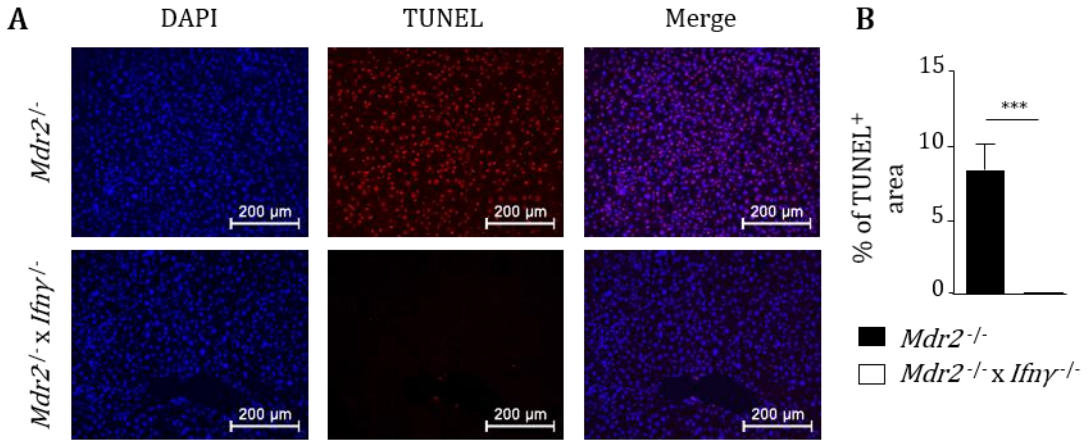

Fig. 18: Liver cell death was diminished in the *Mdr2*$^{-/-}$ x *IFNg*$^{-/-}$ mice. Liver cell death in the *Mdr2*$^{-/-}$ mice and *Mdr2*$^{-/-}$ x *IFNg*$^{-/-}$ mice was visualized using TUNEL staining. Cell nuclei were stained with DAPI. Data: mean values ± SEM, n = 5 (mice), ns: not significant, *p ≤ 0.05, ** p ≤ 0.01. Adapted from Ravichandran *et al*., 2019.

Following analysis of cytotoxicity and cell death, the macrophage populations in C57BL/6 WT mice, *Mdr2*$^{-/-}$ mice, and *Mdr2*$^{-/-}$ x *IFNg*$^{-/-}$ mice were investigated, since these antigen-presenting cells are known to be primed by IFNγ (33). Recently, pro-inflammatory macrophages were identified to be critical in liver injury and fibrosis in mouse models of sclerosing cholangitis (62). Consequently, the myeloid cell populations defined as $CD3^-$ $CD19^-$ $CD11c^-$ $NKp46^-$ $CD11b^+$ $CCR2^{+/-}$ $CX3CR1^{+/-}$, were analyzed by flow cytometry. According to the literature, $CD11b^+$ $CCR2^+$ $CX3CR1^{+/-}$ macrophages were classified as

infiltrating pro-inflammatory monocyte-derived macrophages, whereas CD11b$^+$ CX3CR1$^+$ macrophages were defined as anti-inflammatory and restorative macrophages (62).

Compared to WT mice *Mdr2*$^{-/-}$ mice had increased percentages of pro-inflammatory macrophages, which were defined as CCR2$^+$ CX3CR1$^{+/-}$ as previously described, while the frequency of CX3CR1$^+$ macrophages was reduced. *Mdr2*$^{-/-}$ x *IFNg*$^{-/-}$ mice on the contrary, which lack IFNγ, showed enhanced frequencies of CX3CR1$^+$ restorative macrophages and decreased levels of pro-inflammatory macrophages similar to healthy controls (Fig. 19 A). Moreover, the hepatic expression of *Ccl2*, a potent chemokine attracting monocytes, macrophages and immune cells to the site of injury, was highly up-regulated in *Mdr2*$^{-/-}$ mice compared to WT and *Mdr2*$^{-/-}$ x *IFNg*$^{-/-}$ mice (Fig. 19 B). In summary, whereas *Mdr2*$^{-/-}$ mice displayed increased number of pro-inflammatory macrophages and enhanced expression of *Ccl2*, in *Mdr2*$^{-/-}$ x *IFNg*$^{-/-}$ mice the anti-inflammatory restorative macrophages prevailed.

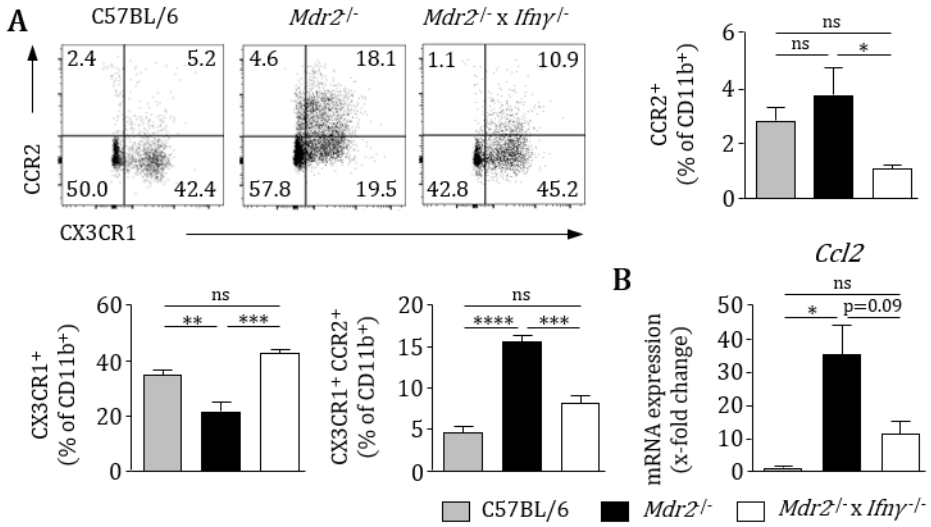

Fig. 19: The restorative macrophages are more prominent in the *Mdr2*$^{-/-}$ x *IFNg*$^{-/-}$ mice (A) CCR2 and CX3CR1 expression of CD11b$^+$ cells were shown in representative dot plots for the different genotypes: C57BL/6 WT mice, *Mdr2*$^{-/-}$ mice and *Mdr2*$^{-/-}$ x *IFNg*$^{-/-}$ mice. The frequencies of CCR2$^+$, CX3CR1$^+$ and CX3CR1$^+$ CCR2$^+$ macrophages were depicted after quantitative analyses. **(B)** The hepatic mRNA expression of *Ccl2* was determined by qRT-PCR. Data: mean values ± SEM, n = 5 (mice), ns: not significant, *p ≤ 0.05, ** p ≤ 0.01. Adapted from Ravichandran *et al*., 2019.

On the basis of the findings in *Mdr2*$^{-/-}$ x *IFNg*$^{-/-}$ mice such as reduced infiltration of lymphocytes, compromised cytotoxicity of CD8$^+$ T cells and NK cells as well as reduced frequency of pro-inflammatory macrophages, IFNγ-deficiency was suspected to have an impact on the immune pathogenesis of PSC. Based on these results, the pathology of the *Mdr2*$^{-/-}$ x *IFNg*$^{-/-}$ mice was analyzed.

However, the biliary inflammation in *Mdr2*$^{-/-}$ x *IFNg*$^{-/-}$ mice was not changed compared to *Mdr2*$^{-/-}$ mice. ALT levels were similar to *Mdr2*$^{-/-}$ mice, even if AST levels were significantly reduced in *Mdr2*$^{-/-}$ x *IFNg*$^{-/-}$ mice compared to *Mdr2*$^{-/-}$ mice (Fig. 20 A). In addition, the mHAI score displayed no differences in liver inflammation between both genotypes (Fig. 20 B). Nevertheless, regarding fibrosis, reduced collagen deposition in the livers of *Mdr2*$^{-/-}$ x *IFNg*$^{-/-}$ mice was detected in comparison to *Mdr2*$^{-/-}$ mice (Fig. 20 C-E). Consequently, ablation of IFNγ in a mouse model of chronic liver inflammation fails to show improvement of tissue damage but attenuates fibrosis.

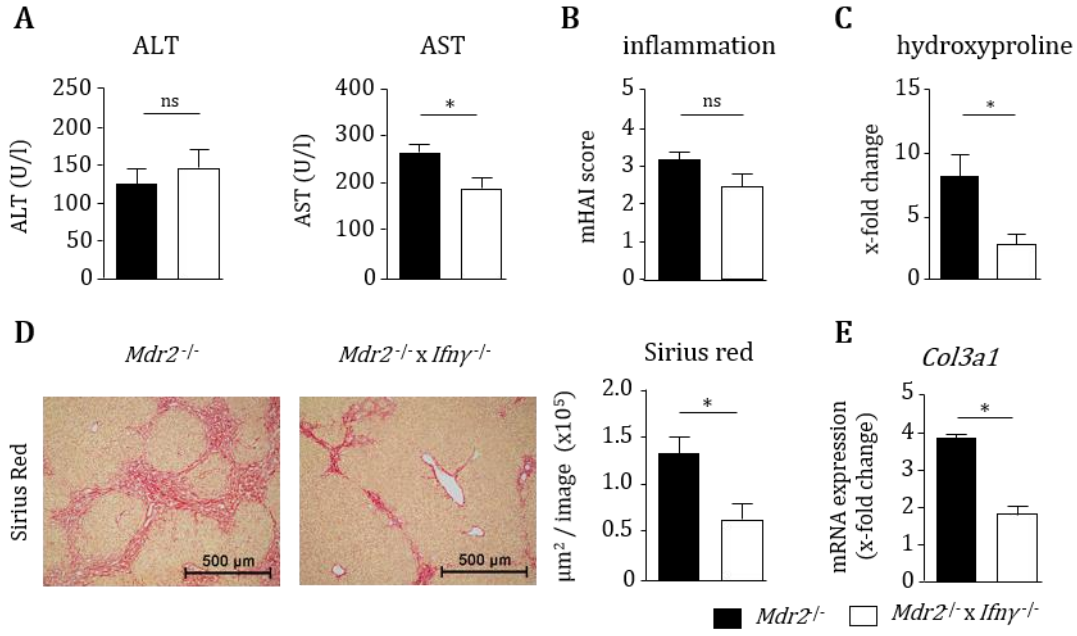

Fig. 20: *Mdr2*$^{-/-}$ x *IFNg*$^{-/-}$ mice showed reduced fibrosis compared to *Mdr2*$^{-/-}$ mice. Liver inflammation and fibrosis of *Mdr2*$^{-/-}$ mice were compared to *Mdr2*$^{-/-}$ x *IFNg*$^{-/-}$ mice. **(A)** Activity of the liver enzymes ALT and AST were measured in the plasma. **(B)** The liver inflammation measured by the mHAI score was determined. **(C)** The relative Hyp content in livers of the *Mdr2*$^{-/-}$ x *IFNg*$^{-/-}$ mice and *Mdr2*$^{-/-}$ mice was quantified. **(D)** Sirius Red positive area was analyzed in liver sections. **(E)** Hepatic mRNA expression of *Col3a1* was determined by qRT-PCR. Data: mean values ± SEM, n = 5 (mice), ns: not significant, *p ≤ 0.05, ** p ≤ 0.01. Adapted from Ravichandran *et al*., 2019.

3.7. Neutralisation of IFNγ attenuated fibrosis in *Mdr2*$^{-/-}$ mice

According to the results of *Mdr2*$^{-/-}$ x *IFNg*$^{-/-}$ mice analyses, IFNγ-deprivation entailed various effects including reduced hepatic cell death and attenuated fibrosis. As a consequence, an engagement of IFNγ in the immune pathogenesis of PSC is very likely and neutralization of IFNγ might display a new therapeutic approach in chronic liver inflammation. In order to verify this concept, 10-week-old *Mdr2*$^{-/-}$ mice were treated twice a week over a period of 14 days with anti-IFNγ Ab or isotype control.

The anti-IFNγ Ab treatment in *Mdr2*$^{-/-}$ mice had no effects on tissue damage and inflammation, since ALT levels and mHAI score were similar in both treatment groups (Fig. 21 A). Nonetheless, fibrosis was significantly decreased in the anti-IFNγ Ab-treated mice, as shown by the relative Hyp content, Sirius red staining and hepatic *Col3A1* expression (Fig. 21 B) similar to *Mdr2*$^{-/-}$ x *IFNg*$^{-/-}$ mice. Taken together, treatment of *Mdr2*$^{-/-}$ mice with anti- IFNγ Ab results in reduced fibrosis.

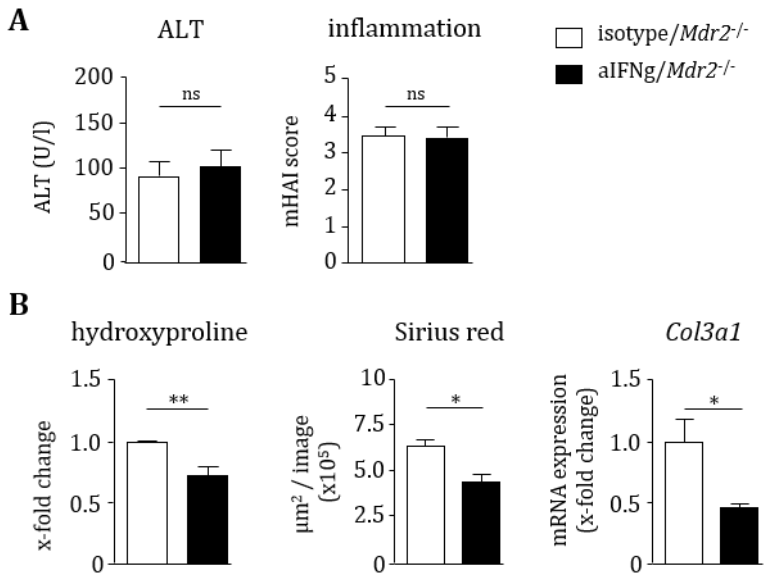

Fig. 21: Anti-IFNγ treatment in the *Mdr2*$^{-/-}$ mice had no effect on tissue damage, but reduced fibrosis. 10-week-old *Mdr2*$^{-/-}$ mice were treated twice a week over a period of 14 days with anti-IFNγ Ab or isotype control. **(A)** Plasma ALT levels were determined, and liver inflammation was calculated using mHAI score. **(B)** Fibrosis was determined by Hyp content, Sirius Red staining and the hepatic mRNA expression of *Col3a1*. Data: mean values ± SEM, n = 5 (mice), ns: not significant, *p ≤ 0.05, ** p ≤ 0.01. Adapted from Ravichandran *et al*., 2019.

4. Discussion

Although PSC ranks as a rare disease, its incidence increases worldwide (20). No adequate treatments for PSC are currently available, demonstrating the urgent need for new therapeutic interventions. In the worst case, PSC progresses via different stages to end-stage liver failure, which requires liver transplantation. So far, insights into the underlying mechanisms of the disease are elusive which hampers the development of new therapies. In this study, we focused on the analysis of the role of IFNγ in the immune pathogenesis of PSC in order to unfold the mechanisms leading to biliary inflammation and liver fibrosis.

First hints that this pleiotropic cytokine might be involved in disease progression were the accumulation of Th1 cells around bile ducts (6) and enhanced expression of downstream molecules of IFNγ signaling pathway in the livers of PSC patients (32). Additionally, we have been able to show increased levels of IFNγ and IFNγ-inducible chemokines CXCL10 and CXCL11 in the sera of PSC patients (5). Likewise, *Mdr2*$^{-/-}$ mice, which resemble human PSC and were used in this study to analyze the underlying mechanism of PSC progression, also showed increased production of IFNγ by CD8^{+} T cells and NKT cells and elevated hepatic mRNA expression of IFNγ-induced chemokines *Cxcl9* and *Cxcl10*. These findings point to the relevance of IFNγ not only in human PSC but also in the mouse model of sclerosing cholangitis and further underscores the necessity to analyze the role of IFNγ in PSC progression. In addition, increased frequencies of CD8^{+} T cells, NKT cells and NK cells in the livers of *Mdr2*$^{-/-}$ mice emphasized the role of IFNγ-producing cells in chronic liver inflammation. Accumulation of these cells in the liver might result from enhanced levels of CXCL9 and CXCL10. These chemokines attract immune cells to the inflammatory site by binding to their corresponding chemokine receptor CXCR3 expressed on various cells including Th1 cells, CD8^{+} T cells, NKT cells and NK cells (63).

As a result of T cell depletion, which primarily affected CD4^{+} T cells, CD8^{+} T cells and NKT cells, while the number of NK cells was only partly reduced, we could show diminished levels of pro-inflammatory cytokines IFNγ, IL-17A, TNFα and IL-2. This result highlights T cells in general as the primary source of pro-inflammatory cytokines in *Mdr2*$^{-/-}$ mice. Moreover, compromised NK cell cytotoxicity was another consequence of T cell depletion, which can occur due to limited cytokine availability. NK cell activation was shown to

depend on IL-2 as well as on IFNs (28) and thus, reduced levels of these cytokines might reduce NK cell activation, and therefore cytotoxicity.

Furthermore, following anti-Thy1.2 Ab treatment in the *Mdr2*$^{-/-}$ mice, liver injury was reduced, pinpointing an involvement of T cells in biliary inflammation. However, fibrosis was not affected in response to T cell depletion. Since the same results were obtained from *Mdr2*$^{-/-}$ x *Rag1*$^{-/-}$ mice, which lack T and B cells, T cells might be considered as mediators of liver injury in *Mdr2*$^{-/-}$ mice, but at the same time as non-essential in the process of fibrogenesis.

The analysis of the leukocytic composition of explant livers of PSC and control patients in turn revealed no differences in the T cell compartment, but an increased frequency of CD56^{+} NK cells, especially of CD56^{bright} NK cells in PSC patients. CD56^{bright} NK cells are described in literature as displaying tissue-resident phenotype (61). Additionally, the NK cells showed a bias towards increased TRAIL expression, indicating enhanced cytotoxic functions. Based on these findings, cytotoxic NK cells might be of relevance to the immune pathogenesis of PSC. The lack of attenuation of fibrosis following T cell depletion in *Mdr2*$^{-/-}$ mice and in *Mdr2*$^{-/-}$ x *Rag1*$^{-/-}$ mice might be due to NK cells, which are potent IFNγ producers and were still present in these mice.

This assumption is in line with genomic association studies proposing NK cell-related genes as candidate loci for disease susceptibility in PSC (26). These genetic variants were located primarily within the HLA complex, triggering, among other functions, NK cell activation. In general, activation of NK cells is based on the interplay of activating and inhibitory receptors and hence, imbalance in the signaling might lead to reduced inhibition and /or increased activation of NK cells and finally to auto-reactivity (64). According to this study, the frequencies of HLA-Bw4 and –C2, a HLA class I ligand of the inhibitory Killer-cell immunoglobulin-like receptors (KIRs) 3DL1 and 2DL1, were reduced in PSC patients (26). Additionally, the ligand of the activating NKG2D receptor major histocompatibility complex class I chain-related A (*MICA*008*) molecule was found to act as a recessive risk allele in PSC patients (65). These findings implicate the involvement of dysfunctional NK cells in PSC. Hence, it seems likely that NK cells play a role in the immune pathogenesis of PSC.

Depletion of NK cells using anti-asialo GM1 Ab in *Mdr2*$^{-/-}$ mice led to the down-regulation of IFNγ and cytotoxic markers GzmB and TRAIL in CD8^{+} T cells, pointing to an involvement

of NK cells in $CD8^+$ T cell activation. Several studies have demonstrated the interaction of NK cells and dendritic cells (DCs) in the activation process of $CD8^+$ T cells. During viral infections, NK cells were found to activate Th1 and $CD8^+$ T cell responses by triggering DC activation and promoting DC-driven polarization of $CD8^+$ T cells and Th1 cells (66). Moreover, NK cells were also shown to interact with $CD8^+$ T cells directly, as shown in hepatitis B virus (HBV) infection. Upon infection, NK cells promoted TRAIL-mediated killing of HBV-specific $CD8^+$ T cells (67,68). However, this mechanism seems to be HBV-specific as it was not observed in case of HCV and Epstein Bar Virus (68). Furthermore, NK cells were found to attract DCs in presence of tumor cells which in response released chemokines, eliciting the recruitment of effector $CD8^+$ T cells into the tumorigenic tissue (69). In summary, these findings point out the role of NK cells in the activation process of $CD8^+$ T cells through stimulation and recruitment of DCs. Accordingly, reduced activity of $CD8^+$ T cells after anti-asialo GM1 Ab treatment might be explained by the absence of NK cells in *Mdr2*$^{-/-}$ mice.

Liver injury was not altered following anti-asialo GM1 Ab treatment in *Mdr2*$^{-/-}$ mice. Since, excepting $CD8^+$ T cells, the functions regarding cytokine production of other T cells were not affected by NK cell depletion, these cells might continue to drive biliary inflammation further. Fibrosis on the other hand was attenuated as a response to the treatment with anti-asialo GM1 Ab. Consequently, these data encourage the assumption that NK cells play a role in the process of fibrogenesis. As part of the innate immune system, NK cells are characterized by their cytotoxic ability and cytokine and chemokine secretion, with IFNγ as their main effector cytokine (64). The function of NK cells or rather IFNγ in fibrosis has been discussed controversially. Until recently, IFNγ was reported to have mainly anti-fibrotic functions. Radaeva et al., suggested an anti-fibrotic effect of NK cells in liver fibrosis by IFNγ or polyinosinic-polycytidylic acid-induced killing of hepatic stellate cells in NKG2D- and TRAIL-dependent manner (24). Moreover, an anti-fibrotic effect of IFNγ was also observed in HBV-infected patients after administration of IFNγ for 9 months. Analysis of the phenomenon revealed amelioration of liver fibrosis following IFNγ treatment via phosphorylation of STAT-1, upregulation of Smad7 expression and impaired TGF-β signaling in hepatic stellate cells *in vitro* (70). Similar results were gathered in experimental models of pulmonary and kidney fibrosis (71). Nevertheless, besides anti-fibrotic effects, some publications also reported pro-fibrotic functions of IFNγ. In a mouse model of steatohepatitis induced by a methionine- and choline-deficient

high fat diet, IFNγ was proposed to induce the inflammatory response of macrophages and subsequently to initiate hepatic stellate cell activation and liver fibrosis (23). In addition, the interaction of IFNγ with hepatic progenitor cells (HPC) was also described to enhance HPC response to injury and to stimulate hepatic inflammation and aggravate liver damage (72). Furthermore, IFNγ-producing $CD56^{bright}$ NK cells have already been shown to play a role in tubulointerstitial fibrosis in chronic kidney disease (73). In summary, a contribution of NK cells or their effector cytokine IFNγ to liver fibrosis is likely, since in our study the depletion of NK cells in *Mdr2*$^{-/-}$ mice resulted in reduced IFNγ production, reduced cytotoxicity of $CD8^+$ T cells and impaired fibrosis.

In order to analyze the impact of IFNγ in the immune pathogenesis of PSC *Mdr2*$^{-/-}$ x *IFNg*$^{-/-}$ mice were analyzed. In *Mdr2*$^{-/-}$ x *IFNg*$^{-/-}$ mice, frequencies of hepatic $CD4^+$ T cells, $CD8^+$ T cells, NKT cells, $TCR\gamma\delta^+$ T cells, and NK cells were reduced, as was mRNA expression of IFNγ-induced chemokines *Cxcl9* and *Cxcl10* compared to *Mdr2*$^{-/-}$ mice. Reduced lymphocytic frequencies might be a consequence of decreased chemokine levels leading to compromised recruitment, which emphasizes the importance of IFNγ in the process of attraction and migration of immune cells into the inflamed tissue.

Additionally, in *Mdr2*$^{-/-}$ x *IFNg*$^{-/-}$ mice we observed down-regulation of the cytotoxic markers GzmB and TRAIL in NK and $CD8^+$ T cells compared to *Mdr2*$^{-/-}$ mice. Subsequently, while the cytotoxic capacities of $CD8^+$ T cells and NK cells were highly elevated in chronic liver inflammation, in absence of IFNγ the cytotoxicity of these cells was significantly reduced. These results suggest a dependence on IFNγ regarding the cytotoxic capacities of $CD8^+$ T cells and NK cells. The pro-apoptotic effect of IFNγ is well-known. Among other functions, IFNγ was reported to up-regulate the expression of various apoptosis-related proteins, such as TNF-R1, CD95 and other death receptors and their corresponding ligands, and caspases, which are crucial for the induction of apoptosis in target cells (74–76). Bhat and colleagues have described autocrine production of IFNγ to be essential for the enhancement of motility and target killing of $CD8^+$ T cells (77). Moreover, IFNγ was found to sensitize target cells towards TRAIL-induced apoptosis by blocking the up-regulation of TRAIL-induced IAP-2 (78) as well as through Interferon regulatory factor 1 (IRF-1) expression (79). IFNγ has also been noted to promote TRAIL-induced cell death by increasing the expression of caspase-8 (80). According to Sedger et al., IFNγ was described to decrease the basal level of NF-κB activation, which acts as survival factor,

and to balance the TRAIL and TRAIL-R expression in order to induce targeted apoptosis following CMV infection (81). Apart from that, in the context of graft-versus-tumor, IFNγ was associated with enhanced activation of cytotoxic T cells and increased production of GzmB (82). All these facts support the assumption of an involvement of IFNγ in the induction of cytotoxic functions and consequently provide an explanation for reduced production of GzmB and TRAIL in *Mdr2*$^{-/-}$ x *IFNg*$^{-/-}$ mice. In summary, the results suggest that IFNγ is not only involved in the recruitment of immune cells to the site of inflammation, but also in the induction of cytotoxicity of NK cells and CD8^{+} T cells in murine sclerosing cholangitis.

Also, regarding PSC, the cytotoxicity has been found to be of importance. Takeda et al., described TRAIL-R/DR5 (Death receptor 5) to be the key regulator of cholestatic liver injury, which also includes PSC (83). The treatment of C57BL/6 mice with the agonistic anti-DR5 Ab resulted in apoptosis of cholangiocytes and subsequently in cholestatic liver injury with a histological appearance reminiscent of human PSC. Moreover, in addition to enhanced apoptosis of cholangiocytes in PSC patients, these cells are as well described to express DR5 and increased levels of TRAIL (83). Thus, TRAIL or cytotoxicity in general can be assumed to play an important part in the induction of cell death of cholangiocytes and to drive liver inflammation in PSC.

Analysis of cell death in *Mdr2*$^{-/-}$ mice displayed massive accumulation of apoptotic cells within the liver, which correlated with increased expression of cytotoxic markers in CD8^{+} T cells and NK cells. Then again, in absence of IFNγ apoptotic cells were almost absent, as were the cytotoxic capacities of CD8^{+} T cells and NK cells. Hence, we can conclude that cytotoxicity seems to be linked to induction of apoptosis. Similarly, in the mouse model of Concanavalin-A induced hepatitis IFNγ deficiency was described to suppress hepatic injury by reducing Fas-induced apoptosis of liver cells (84). Nevertheless, IFNγ might also act directly on hepatocytes and induce apoptosis, since it has been described to induce cell cycle arrest and p-53 independent apoptosis in primary cultured hepatocytes with IRF-1 as the key regulator (85). Hence, independently of a direct effect of IFNγ on hepatocytes or indirect activation of pro-apoptotic molecules by this cytokine, IFNγ seems to be involved in the hepatocyte death in experimental sclerosing cholangitis.

However, it is important to keep in mind that in Mdr2$^{-/-}$ mice apoptosis of hepatocytes can be induced by toxic bile acids (51). Hence, the impact of IFNγ in this setting is still elusive.

First hints for an interaction between BA and cytotoxicity were obtained by Gores and co-workers. They proposed BA-induced apoptosis of hepatocytes in a FAS- and TRAIL-dependent manner (86). And since IFNγ is involved in the sensitization of target cells towards TRAIL-mediated cytotoxicity, the lack of IFNγ in turn might reduce BA-induced apoptosis of hepatocytes.

Finally, enhanced hepatocellular damage leads to increased formation of endogenous stress signals inducing activation of macrophages (49). Basically, the activation of macrophages is a two step-process. The first signal is IFNγ, which acts as initiating factor. The second step are the endogenous signals, referred to as pathogen-associated molecular patterns or damage-associated molecular patterns (DAMPs), that bind to TLR expressed on macrophages. In response to this activation, macrophages undergo physiological changes and produce cytokines, chemokines and toxic mediators in order to initiate inflammatory responses (49,71). Macrophages are a highly heterogeneous cell population with ambivalent functions in the progression of chronic inflammation. They differentiate in response to micro-environmental conditions towards pro-inflammatory or anti-inflammatory phenotypes. They are commonly characterized as pro-inflammatory classical macrophages (M1-like) and anti-inflammatory alternative macrophages (M2-like) (87). However, due to their high plasticity the strict separation by their phenotype is very difficult.

In the context of fibrosis, macrophages were described to promote the progression of fibrosis via secretion of pro-inflammatory factors and maintaining NF-κB activation in the early stage. In the late stage on the other hand it has been suggested that the cells foster the resolution of hepatic fibrosis through the secretion of matrix metalloproteinases (87). In the model of sclerosing cholangitis as well as in PSC samples, Guicciardi et al. could show an increased number of peribiliary macrophages (62). Even though both types of macrophages were represented, the pro-inflammatory monocyte-derived macrophages prevailed. Blockage of CCR2 reduced the infiltration of circulating monocytes into the liver and reduced biliary injury and fibrosis (62). In our study, we could confirm the enhanced recruitment of $CCR2^{+}$ $CX3CR1^{+/-}$ macrophages in the liver of *Mdr2*$^{-/-}$ mice. In contrast, in *Mdr2*$^{-/-}$ x *IFNg*$^{-/-}$ mice we observed an accumulation of the anti-inflammatory $CX3CR1^{+}$ macrophages in the livers, which are defined to have restorative abilities and to participate in fibrolysis (liver fibrosis regression). Thus, it can be assumed that presence

of IFNγ is necessary to attract pro-inflammatory macrophages to the inflamed tissue. This assumption is supported by the reduced hepatic mRNA expression of *Ccl2*, a chemokine involved in monocyte/macrophage recruitment, in *Mdr2*$^{-/-}$ x *IFNg*$^{-/-}$ mice.

In summary, we can conclude that the pleiotropic cytokine IFNγ does not merely play a single role in the immune pathogenesis of PSC. Instead, it is involved in several processes, all of which are crucial for disease progression. First, IFNγ induces the recruitment of immune cells to the site of inflammation by promoting the production of IFNγ-induced chemokines. The immune cells in turn initiate an inflammatory response leading to biliary inflammation. In addition, IFNγ activates NK cells and intensifies the production of cytotoxic markers triggering cholangiocyte and or hepatocyte death. Finally, the inflammatory macrophages are activated and further promote fibrosis development. In summary, in this study we could show for the first time that IFNγ has a pro-fibrotic effect in the immune pathogenesis of PSC and that targeting this pleiotropic cytokine might represent a new therapeutic option for treatment of PSC.

5. Outlook

In this study we could finally show that IFNγ-dependent immune responses are involved in the immune pathogenesis of PSC. The main producers of IFNγ in *Mdr2*$^{-/-}$ mice are hepatic CD8^{+} T cells and NK cells. In response to elevated IFNγ production, the hepatic expression of IFNγ-inducible chemokines CXCL9 and CXCL10 was highly increased. Moreover, IFNγ was shown to change the phenotype of hepatic CD8^{+} T cells and NK cells towards increased cytotoxicity and to induce cell death of hepatocytes and/or cholangiocytes. In addition, the presence of IFNγ triggered the recruitment of pro-inflammatory monocytes into the inflamed tissue. Ultimately, we could demonstrate the pro-fibrotic functions of this cytokine in liver fibrosis. These data suggest that IFNγ is involved in hepatic effector cell migration and lymphocyte cytotoxicity and hence promotes liver fibrosis.

Since we observed an increased number of CD56^{+} NK cells in the explant livers, and the depletion of NK cells in *Mdr2*$^{-/-}$ mice resulted in reduced cytotoxicity of CD8^{+} T cells and reduced fibrosis, it seems likely these cells play a role in the pathogenesis. Further characterization of the phenotype and the function of NK cells would enable a better understanding of their role in the pathology. Moreover, we identified other IFNγ^{+} cells in *Mdr2*$^{-/-}$ mice, which were neither T cells nor NK cells (data not shown). We suspect these cells to be type 1 innate lymphoid cells (ILC1), which are described to share features of conventional NK cells and to be abundant in the liver (88). Despite some similarities, including potent IFNγ production, the ILC1 differ from NK cells in some respects such as localization, transcriptional regulation and phenotype. They have so far not been considered in our studies but might also be involved in the pathogenesis of PSC. The characterization of ILC1 in addition to NK cells in both PSC explant livers and *Mdr2*$^{-/-}$ mice would provide insights into further mechanisms and lead to a better understanding of the pathophysiology.

Since cytotoxicity of CD8^{+} T cells and NK cells have been shown to be of importance in the progression of PSC, analysis of the *Mdr2*$^{-/-}$ x *GzmB*$^{-/--}$ and *Mdr2*$^{-/-}$ x *Trail*$^{-/-}$ mice would permit analysis of the significance of lymphocyte cytotoxicity in the model of sclerosing cholangitis. In addition, analysis of the downstream signaling pathway of GzmB- and TRAIL-induced apoptosis will establish novel treatment targets, which could be easily manipulated.

Another approach promising enough to be considered is the application of anti-p40 mAb (Ustekinumab; licensed for the treatment of IBD) or the AMG487 antagonists against CXCR3. Ustekinumab blocks IL-12, a key factor for production of IFNγ by T cells. And CXCR3 is a receptor involved in IFNγ-mediated effector cell recruitment for PSC pathology. Blocking the migration of immune cells into the inflamed tissue might have a protective effect and inhibit liver inflammation.

In summary, in this PhD thesis we could collect first hints of a contribution of IFNγ to the immune pathogenesis of PSC. However, the exact mechanisms behind this are still elusive and have yet to be investigated further in order to find new therapeutic approaches.

6. Abstract

Primary sclerosing cholangitis (PSC) is an idiopathic, cholestatic chronic liver disease characterized by biliary inflammation and periductal "onion skin"-type fibrosis. Due to a lack of understanding of the pathophysiology treatment options are limited. According to studies in PSC patients, increased accumulation of T cells, in particular Th1 cells, around bile ducts and elevated levels of IFNγ-induced chemokines in the sera were found, indicating an involvement of IFNγ in disease development and progression. The aim of this thesis was to investigate the role of IFNγ in the immune pathogenesis of PSC. The experiments were conducted in multi-drug resistance protein 2 knockout (*Mdr2*$^{-/-}$) mice, which is an established mouse model resembling human PSC.

First of all, we could show CD8$^+$ T cells and NK cells as the main producers of IFNγ in the *Mdr2*$^{-/-}$ mouse strain. Depletion of CD90.2$^+$ cells, which are mainly T cells, reduced liver inflammation, the production of pro-inflammatory cytokines and NK cell cytotoxicity. However, fibrosis was not affected by T cell depletion. Similar results were obtained from *Mdr2*$^{-/-}$ x *Rag1*$^{-/-}$ mice. Analysis of liver samples from PSC and control patients depicted elevated numbers of TRAIL$^+$ CD56^{bright} NK cells in PSC patients but no differences in the percentage of T lymphocytes. Depletion of NK cells in *Mdr2*$^{-/-}$ mice decreased CD8$^+$ T cell cytotoxicity and IFNγ production and reduced liver fibrosis, while liver injury was not altered. Complete absence of IFNγ in the *Mdr2*$^{-/-}$ x *IFNg*$^{-/-}$ mice reduced the frequencies of CD8$^+$ T cells and NK cells expressing the cytotoxic markers granzyme B and TRAIL. In addition, *Mdr2*$^{-/-}$ x *IFNg*$^{-/-}$ mice displayed elevated frequencies of restorative CX3CR1$^+$ macrophages, while *Mdr2*$^{-/-}$ mice predominantly harbored pro-inflammatory CCR2$^+$CX3CR1$^{+/-}$ macrophages. Furthermore, ablation of IFNγ led to absence of hepatocellular death in comparison to *Mdr2*$^{-/-}$ mice and reduced fibrosis. In a therapeutic approach, the efficiency of anti-IFNγ Ab treatment in chronic liver disorder was also analyzed. Even the application of anti-IFNγ Ab for a short period resulted in reduced fibrosis in *Mdr2*$^{-/-}$ mice.

In summary, we could present in our work the pro-fibrotic properties of IFNγ in PSC. IFNγ changed the phenotype of hepatic CD8$^+$ T cells and NK cells towards increased cytotoxicity and promoted induction of cell death and infiltration of inflammatory macrophages into the inflamed tissue. Therefore, targeting IFNγ in PSC patients might be considered as a therapeutic option.

7. Zusammenfassung

Die primär sklerosierende Cholangitis (PSC) ist eine chronisch verlaufende Entzündung der intra- und extrahepatischen Gallengänge, die zur Cholestase und anschließender Zirrhose führt. Bislang sind die Mechanismen, die der Pathogenese zugrunde liegen, unbekannt, was die therapeutischen Optionen einschränkt. Studien zufolge konnte bei PSC Patienten eine erhöhte Anzahl an T-Zellen, insbesondere Th1 Zellen, in der Nähe der Gallengänge gefunden werden, wie auch erhöhte Mengen an IFNγ-induzierten Chemokine in den Seren. Diese Daten weisen auf eine mögliche Beteiligung der Th1 Zellen und IFNγ an der Entwicklung der Krankheit hin. Ziel der Arbeit ist es, die Rolle von IFNγ in der Immunpathogenese von PSC zu untersuchen. Hierfür werden multidrug resistance protein 2 knockout (*Mdr2*$^{-/-}$) Mäuse verwendet, da sie zusätzlich zu einer chronischen Leberentzündung die für PSC typischen zwiebelschalenartigen Veränderungen der Gallengänge aufweisen.

Zunächst einmal konnte in den *Mdr2*$^{-/-}$ Mäusen die CD8^{+} T Zellen und NK-Zellen als die Hauptproduzenten von IFNγ gezeigt werden. Anschließende Depletion der CD90.2^{+} Zellen, die überwiegend T-Zellen sind, führte zu einer reduzierten Leberentzündung, verminderten Produktion von pro-inflammatorischen Zytokinen und reduzierten NK Zell-Zytotoxizität. Die Behandlung hatte keine Auswirkung auf die Fibrose. Ähnliche Ergebnisse konnten mit den *Mdr2*$^{-/-}$ x *Rag1*$^{-/-}$ Mäusen generiert werden. Die Analysen der Leberproben von PSC- und Kontroll-Patienten zeigten jedoch in Hinblick auf T-Lymphozyten Population keine Unterschiede, aber eine Zunahme von TRAIL^{+} CD56^{bright} NK Zellen bei PSC Patienten. Nachfolgende Depletion der NK Zellen in den *Mdr2*$^{-/-}$ Mäusen führte wiederum zu verringerter CD8^{+} T Zell-Zytotoxizität und IFNγ Produktion und verbesserter Fibrose. In den *Mdr2*$^{-/-}$ x *IFNg*$^{-/-}$ Mäusen dagegen bedingte die Abwesenheit von IFNγ die Herabregulation der zytotoxischen Marker Granzym B und TRAIL in CD8^{+} T Zellen und NK Zellen. Außerdem konnte in diesen Mäusen eine erhöhte Frequenz an CX3CR1^{+} restorativen Makrophagen beobachtet werden, wohingegen in *Mdr2*$^{-/-}$ Mäusen pro-inflammatorische CCR2^{+} CX3CR1$^{+/-}$ Makrophagen überwiegten. Zudem führt das Fehlen von IFNγ zu stark verringertem Zelltod von Hepatozyten und reduzierter Fibrose. Zuletzt wurde die therapeutische Anwendung von anti-IFNγ Antikörpern bei der chronischen Leberentzündung untersucht. Die Neutralisation von IFNγ führte zu einer verringerten Fibrose wie bei den *Mdr2*$^{-/-}$ x *IFNg*$^{-/-}$ Mäusen.

Zusammenfassend konnte in dieser Arbeit die pro-fibrotische Wirkung von IFNγ im chronischen Modell der Leberentzündung gezeigt werden. IFNγ erhöht nicht nur die zytotoxische Kapazität von $CD8^+$ T Zellen und NK Zellen, sondern ist auch an der Induktion von Apoptose in Hepatozyten und Rekrutierung von pro-inflammatorischen Makrophagen in das Gewebe beteiligt. Daher könnte die Neutralisierung von IFNγ eine mögliche Therapieoption darstellen.

References

1. Konturek P, Harsch I, Konturek K, Schink M, Konturek T, Neurath M, u. a. Gut–Liver Axis: How Do Gut Bacteria Influence the Liver? Med Sci. 2018;6(3):79.

2. SKURKOVICH S V, KLINOVA EG, EREMKINA EI, LEVINA N V. Immunosuppressive Effect of an Anti-interferon Serum. Nature. 1974;247(5442):551–2.

3. Skurkovich S, Skurkovich B, Kelly J. Anticytokine therapy, particularly anti-IFN-γ, in Th1-mediated autoimmune diseases. Expert Rev Clin Immunol. 2005;1(1):11–25.

4. Ravichandran G, Neumann K, Berkhout LK, Weidemann S, Langeneckert AE, Schwinge D, u. a. Interferon-γ-dependent immune responses contribute to the pathogenesis of sclerosing cholangitis in mice. J Hepatol. 2019;71(4):773–82.

5. Langeneckert AE, Lunemann S, Martrus G, Salzberger W, Hess LU, Ziegler AE, u. a. CCL21-expression and accumulation of CCR7 + NK cells in livers of patients with primary sclerosing cholangitis. Eur J Immunol. 2019;49(5):758–69.

6. Landi A, Weismuller TJ, Lankisch TO, Santer DM, Tyrrell DLJ, Manns MP, u. a. Differential serum levels of eosinophilic eotaxins in primary sclerosing cholangitis, primary biliary cirrhosis, and autoimmune hepatitis. J Interf Cytokine Res. 2014;34(3):204–14.

7. Heubi JE. Bile Acid Physiology and Alterations in the Enterohepatic Circulation. Pediatr Gastrointest Liver Dis. 1. Januar 2011;20-27.e2.

8. Trefts E, Gannon M, Wasserman DH. The liver. Current Biology. 2017.

9. Michalopoulos GK. Liver regeneration. J Cell Physiol. November 2007;213(2):286–300.

10. Qin L, Qin L, Crawford JM, Sanyal AJ, Boyer TD, Lindor KD, u. a. Anatomy and Cellular Functions of the Liver. 2012. 0–2 S.

11. Gray H, Lewis WH. Anatomy of the human body. Philadelphia: Lea & Febiger; 1918.

12. Roberts MS, Magnusson BM, Burczynski FJ, Weiss M. Enterohepatic circulation: Physiological, pharmacokinetic and clinical implications. Clin Pharmacokinet. 2002;41(10):751–90.

13. Tremaroli V, Bäckhed F. Functional interactions between the gut microbiota and host metabolism. Nature. 2012;489(7415):242–9.

14. Kho ZY, Lal SK. The human gut microbiome - A potential controller of wellness and disease. Front Microbiol. 2018;9(AUG):1–23.

15. Karlsen TH, Folseraas T, Thorburn D, Vesterhus M. Primary sclerosing cholangitis – a comprehensive review. J Hepatol. 1. Dezember 2017;67(6):1298–323.

16. Pontecorvi V, Carbone M, Invernizzi P. The „gut microbiota“ hypothesis in primary

sclerosing cholangitis. Ann Transl Med. Dezember 2016;4(24):512.

17. Lederberg, J. and McCray AT. Omics—A Genealogical Treasury of Words. Scientist. 2001;15(8):7.

18. Sabino J, Vieira-silva S, Machiels K, Joossens M, Falony G, Ballet V, u. a. Primary sclerosing cholangitis is characterised by intestinal dysbiosis independent from IBD. Gut. 2016;65:1681–9.

19. European Association for the Study of the Liver. EASL Clinical Practice Guidelines: Management of cholestatic liver diseases. J Hepatol. 1. August 2009;51(2):237–67.

20. Lazaridis KN, LaRusso NF. Primary Sclerosing Cholangitis. N Engl J Med. 22. September 2016;375(12):1161–70.

21. Gidwaney NG, Pawa S, Das KM. Pathogenesis and clinical spectrum of primary sclerosing cholangitis. World J Gastroenterol. 2017;23(14):2459–69.

22. Jiang X, Karlsen TH. Genetics of primary sclerosing cholangitis and pathophysiological implications. Nat Rev Gastroenterol Hepatol. 2017;14(5):279–95.

23. Nakamoto N, Sasaki N, Aoki R, Miyamoto K, Suda W, Teratani T, u. a. Gut pathobionts underlie intestinal barrier dysfunction and liver T helper 17 cell immune response in primary sclerosing cholangitis. Nat Microbiol. 2019;4(3):492–503.

24. Pellicoro A, Ramachandran P, Iredale JP, Fallowfield JA. Liver fibrosis and repair: Immune regulation of wound healing in a solid organ. Nat Rev Immunol. 2014;14(3):181–94.

25. Bataller R, Brenner DA. Liver fibrosis. J Clin Invest. Februar 2005;115(2):209–18.

26. Karlsen TH, Boberg KM, Olsson M, Sun JY, Senitzer D, Bergquist A, u. a. Particular genetic variants of ligands for natural killer cell receptors may contribute to the HLA associated risk of primary sclerosing cholangitis. J Hepatol. 2007;46(5):899–906.

27. Chung BK, Hirschfield GM. Immunogenetics in primary sclerosing cholangitis. Curr Opin Gastroenterol. 2017;33(2):93–8.

28. Schoknecht T, Schwinge D, Stein S, Weiler-Normann C, Sebode M, Mucha S, u. a. CD4 + T cells from patients with primary sclerosing cholangitis exhibit reduced apoptosis and down-regulation of proapoptotic Bim in peripheral blood . J Leukoc Biol. 2017;101(2):589–97.

29. Sebode M, Peiseler M, Franke B, Schwinge D, Schoknecht T, Wortmann F, u. a. Reduced FOXP3+ regulatory T cells in patients with primary sclerosing cholangitis are associated with IL2RA gene polymorphisms. J Hepatol. 1. Mai 2014;60(5):1010–6.

30. Dienes HP, Lohse AW, Gerken G, Schirmacher P, Gallati H, Löhr HF, u. a. Bile duct epithelia as target cells in primary biliary cirrhosis and primary sclerosing cholangitis. Virchows Arch. August 1997;431(2):119–24.

31. Liaskou E, Jeffery LE, Trivedi PJ, Reynolds GM, Suresh S, Bruns T, u. a. Loss of CD28 Expression by Liver-Infiltrating T Cells Contributes to Pathogenesis of Primary Sclerosing Cholangitis. Gastroenterology. 1. Juli 2014;147(1):221-232.e7.

32. Mueller T, Beutler C, Picó AH, Shibolet O, Pratt DS, Pascher A, u. a. Enhanced innate immune responsiveness and intolerance to intestinal endotoxins in human biliary epithelial cells contributes to chronic cholangitis. Liver Int. 2011;31(10):1574–88.

33. Schroder K, Hertzog PJ, Ravasi T, Hume DA. Interferon-gamma: an overview of signals, mechanisms and functions. J Leukoc Biol. Februar 2004;75(2):163–89.

34. Green DS, Young HA, Valencia JC. Current prospects of type II interferon γ signaling and autoimmunity. J Biol Chem. 2017/06/26. 25. August 2017;292(34):13925–33.

35. Ellis TN, Beaman BL. Interferon-gamma activation of polymorphonuclear neutrophil function. Immunology. Mai 2004;112(1):2–12.

36. Kelchtermans H, Billiau A, Matthys P. How interferon-γ keeps autoimmune diseases in check. Trends Immunol. 2008;29(10):479–86.

37. Backlund J, Li C, Jansson E, Carlsen S, Merky P, Nandakumar K-S, u. a. C57BL/6 mice need MHC class II Aq to develop collagen-induced arthritis dependent on autoreactive T cells. Ann Rheum Dis. Juli 2013;72(7):1225–32.

38. Wildbaum G, Zohar Y, Karin N. Antigen-specific CD25-Foxp3-IFN- γhighCD4+ T cells restrain the development of experimental allergic encephalomyelitis by suppressing Th17. Am J Pathol. 2010;176(6):2764–75.

39. Raphael I, Nalawade S, Eagar TN, Forsthuber TG. T cell subsets and their signature cytokines in autoimmune and inflammatory diseases. Cytokine. 1. Juli 2015;74(1):5–17.

40. Kalia V, Sarkar S. Regulation of Effector and Memory CD8 T Cell Differentiation by IL-2-A Balancing Act. Front Immunol. 2018;9(December):2987.

41. Gao B, Radaeva S, Park O. Liver natural killer and natural killer T cells: immunobiology and emerging roles in liver diseases. J Leukoc Biol. 2009;86(3):513–28.

42. Sebode M, Schramm C. Natural killer T cells: Novel players in biliary disease? Hepatology. 2015;62(4):999–1000.

43. Rajoriya N, Fergusson J, Leithead JA, Klenerman P. Gamma delta T-lymphocytes in hepatitis C and chronic liver disease. Front Immunol. 2014;5(AUG):1–9.

44. Mah AY, Cooper MA. Metabolic regulation of natural killer cell IFN-γ production. Crit Rev Immunol. 2016;36(2):131–47.

45. Smyth MJ, Cretney E, Kelly JM, Westwood JA, Street SEA, Yagita H, u. a. Activation of NK cell cytotoxicity. Mol Immunol. 2005;42(4 SPEC. ISS.):501–10.

46. Thorburn A. Tumor necrosis factor-related apoptosis-inducing ligand (TRAIL) pathway signaling. J Thorac Oncol. 2007;2(6):461–5.

47. Topham NJ, Hewitt EW. Natural killer cell cytotoxicity: How do they pull the trigger? Immunology. 2009;128(1):7–15.

48. Alter G, Malenfant JM, Altfeld M. CD107a as a functional marker for the identification of natural killer cell activity. J Immunol Methods. 2004;294(1–2):15–22.

49. Zhang X, Mosser DM. Macrophage activation by endogenous danger signals. J Pathol. Januar 2008;214(2):161–78.

50. Smit JJM, Groen K, Mel CAAM, Ottenhoff R, Roan MA Van, Valk MA Van Der, u. a. Homozygous disruption of the murine MDR2 P-glycoprotein gene leads to a complete absence of phospholipid from bile and to liver disease. Cell. 1993;75(3):451–62.

51. Fickert P, Fuchsbichler A, Wagner M, Zollner G, Kaser A, Tilg H, u. a. Regurgitation of bile acids from leaky bile ducts causes sclerosing cholangitis in Mdr2 (Abcb4) knockout mice. Gastroenterology. 1. Juli 2004;127(1):261–74.

52. Fickert P, Pollheimer MJ, Beuers U, Lackner C, Hirschfield G, Housset C, u. a. Characterization of animal models for primary sclerosing cholangitis (PSC). J Hepatol. 1. Juni 2014;60(6):1290–303.

53. Jacquemin E, Bernard O, Hadchouel M, Cresteil D, De Vree JML, Paul M, u. a. The wide spectrum of multidrug resistance 3 deficiency: From neonatal cholestasis to cirrhosis of adulthood. Gastroenterology. 1. Mai 2001;120(6):1448–58.

54. Jungsuwadee P, Vore ME. Efflux Transporters. Compr Toxicol. 1. Januar 2010;557–601.

55. Karpen HE, Karpen SJ. Bile Acid Metabolism During Development. Fetal Neonatal Physiol. 1. Januar 2017;913-929.e4.

56. Ishak K, Baptista A, Bianchi L, Callea F, De Groote J, Gudat F, u. a. Histological grading and staging of chronic hepatitis. J Hepatol. 1. Juni 1995;22(6):696–9.

57. Bedossa P, Poynard T. An algorithm for the grading of activity in chronic hepatitis C. Hepatology. 1996;24(2):289–93.

58. Uchinami H, Seki E, Brenner DA, D'Armiento J. Loss of MMP 13 attenuates murine hepatic injury and fibrosis during cholestasis. Hepatology. 2006;44(2):420–9.

59. Kollias G, Spanopoulou E, Grosveld F, Ritter M, Beech J, Morris R. Differential regulation of a Thy-1 gene in transgenic mice. Proc Natl Acad Sci. 1987;84(6):1492–6.

60. He HT, Naquet P, Caillol D, Pierres M. Thy-1 supports adhesion of mouse thymocytes to thymic epithelial cells through a Ca2(+)-independent mechanism. J Exp Med. 1. Februar 1991;173(2):515 LP – 518.

61. Harmon C, Robinson MW, Fahey R, Whelan S, Houlihan DD, Geoghegan J, u. a. Tissue-resident Eomes(hi) T-bet(lo) CD56(bright) NK cells with reduced proinflammatory potential are enriched in the adult human liver. Eur J Immunol. September 2016;46(9):2111–20.

62. Guicciardi ME, Trussoni CE, Krishnan A, Bronk SF, Lorenzo Pisarello MJ, O'Hara SP, u. a. Macrophages contribute to the pathogenesis of sclerosing cholangitis in mice. J Hepatol. 1. September 2018;69(3):676–86.

63. Kuo PT, Zeng Z, Salim N, Mattarollo S, Wells JW, Leggatt GR. The Role of CXCR3 and Its Chemokine Ligands in Skin Disease and Cancer. Front Med. 25. September 2018;5:271.

64. Orange JS, Ballas ZK. Natural killer cells in human health and disease. Clin Immunol. 1. Januar 2006;118(1):1–10.

65. Norris S, Kondeatis E, Collins R, Stephens H, Harrison P, Vaughan R, u. a. Mapping MHC-encoded susceptibility and resistance in primary sclerosing cholangitis: The role of MICA polymorphism. Gastroenterology. 1. Mai 2001;120(6):1475–82.

66. Mailliard RB, Son Y-I, Redlinger R, Coates PT, Giermasz A, Morel PA, u. a. Dendritic Cells Mediate NK Cell Help for Th1 and CTL Responses: Two-Signal Requirement for the Induction of NK Cell Helper Function. J Immunol. 1. September 2003;171(5):2366 LP – 2373.

67. Schuch A, Hoh A, Thimme R. The role of natural killer cells and CD8(+) T cells in hepatitis B virus infection. Front Immunol. 2014;5:258.

68. Peppa D, Gill US, Reynolds G, Easom NJW, Pallett LJ, Schurich A, u. a. Up-regulation of a death receptor renders antiviral T cells susceptible to NK cell-mediated deletion. J Exp Med. Januar 2013;210(1):99–114.

69. Wong JL, Berk E, Edwards RP, Kalinski P. IL-18-primed helper NK cells collaborate with dendritic cells to promote recruitment of effector CD8+ T cells to the tumor microenvironment. Cancer Res. August 2013;73(15):4653–62.

70. Weng H, Mertens PR, Gressner AM, Dooley S. IFN-γ abrogates profibrogenic TGF-β signaling in liver by targeting expression of inhibitory and receptor Smads. J Hepatol. 1. Februar 2007;46(2):295–303.

71. Wynn TA, Vannella KM. Macrophages in Tissue Repair, Regeneration, and Fibrosis. Immunity. März 2016;44(3):450–62.

72. Knight B, Lim R, Yeoh GC, Olynyk JK. Interferon-γ exacerbates liver damage, the hepatic progenitor cell response and fibrosis in a mouse model of chronic liver injury. J Hepatol. 1. Dezember 2007;47(6):826–33.

73. Law BMP, Wilkinson R, Wang X, Kildey K, Lindner M, Rist MJ, u. a. Interferon-γ production by tubulointerstitial human CD56bright natural killer cells contributes to renal fibrosis and chronic kidney disease progression. Kidney Int. 2017;92(1):79–88.

74. Ruiz-Ruiz C, Munoz-Pinedo C, Lopez-Rivas A. Interferon-γ treatment elevates caspase-8 expression and sensitizes human breast tumor cells to a death receptor-induced mitochondria-operated apoptotic program. Cancer Res. 2000;60(20):5673–80.

75. Shin EC, Ahn JM, Kim CH, Choi Y, Ahn YS, Kim H, u. a. IFN-gamma induces cell death in human hepatoma cells through a TRAIL/death receptor-mediated

apoptotic pathway. Int J cancer. Juli 2001;93(2):262–8.

76. Ahn E-Y, Pan G, Vickers SM, McDonald JM. IFN-gammaupregulates apoptosis-related molecules and enhances Fas-mediated apoptosis in human cholangiocarcinoma. Int J cancer. August 2002;100(4):445–51.

77. Bhat P, Leggatt G, Waterhouse N, Frazer IH. Interferon-γ derived from cytotoxic lymphocytes directly enhances their motility and cytotoxicity. Cell Death Dis. 2017;8(6):e2836.

78. Park S-Y, Billiar TR, Seol D-W. IFN-γ Inhibition of TRAIL-Induced IAP-2 Upregulation, a Possible Mechanism of IFN-γ-Enhanced TRAIL-Induced Apoptosis. Biochem Biophys Res Commun. 22. Februar 2002;291(2):233–6.

79. Park S-Y, Seol J-W, Lee Y-J, Cho J-H, Kang H-S, Kim I-S, u. a. IFN-gamma enhances TRAIL-induced apoptosis through IRF-1. Eur J Biochem. November 2004;271(21):4222–8.

80. Kim K-B, Choi Y-H, Kim I-K, Chung C-W, Kim BJ, Park Y-M, u. a. POTENTIATION OF FAS- AND TRAIL-MEDIATED APOPTOSIS BY IFN-γ IN A549 LUNG EPITHELIAL CELLS: ENHANCEMENT OF CASPASE-8 EXPRESSION THROUGH IFN-RESPONSE ELEMENT. Cytokine. 1. Dezember 2002;20(6):283–8.

81. Sedger LM, Shows DM, Blanton RA, Peschon JJ, Goodwin RG, Cosman D, u. a. IFN-γ Mediates a Novel Antiviral Activity Through Dynamic Modulation of TRAIL and TRAIL Receptor Expression. J Immunol. 15. Juli 1999;163(2):920 LP – 926.

82. Zhao Q, Tong L, He N, Feng G, Leng L, Sun W, u. a. IFN-gamma mediates graft-versus-breast cancer effects via enhancing cytotoxic T lymphocyte activity. Exp Ther Med. August 2014;8(2):347–54.

83. Takeda K, Kojima Y, Ikejima K, Harada K, Yamashina S, Okumura K, u. a. Death receptor 5 mediated-apoptosis contributes to cholestatic liver disease. Proc Natl Acad Sci. 5. August 2008;105(31):10895 LP – 10900.

84. Tagawa Y, Sekikawa K, Iwakura Y. Suppression of concanavalin A-induced hepatitis in IFN-gamma(-/-) mice, but not in TNF-alpha(-/-) mice: role for IFN-gamma in activating apoptosis of hepatocytes. J Immunol. 1. August 1997;159(3):1418 LP – 1428.

85. Kano A, Haruyama T, Akaike T, Watanabe Y. IRF-1 is an essential mediator in IFN-γ-induced cell cycle arrest and apoptosis of primary cultured hepatocytes. Biochem Biophys Res Commun. 1999;

86. Higuchi H, Bronk SF, Takikawa Y, Werneburg N, Takimoto R, El-Deiry W, u. a. The Bile Acid Glycochenodeoxycholate Induces TRAIL-Receptor 2/DR5 Expression and Apoptosis. J Biol Chem. 2001;276(42):38610–8.

87. Li H, You H, Fan X, Jia J. Hepatic macrophages in liver fibrosis: pathogenesis and potential therapeutic targets. BMJ Open Gastroenterol. 2016;3(1):1–4.

88. Luci C, Vieira E, Perchet T, Gual P, Golub R. Natural Killer Cells and Type 1 Innate Lymphoid Cells Are New Actors in Non-alcoholic Fatty Liver Disease . Bd. 10, Frontiers in Immunology . 2019. S. 1192.

Danksagung

In den letzten Jahren hatte ich die Gelegenheit ein wissenschaftliches Projekt zu bearbeiten und mich im Bereich der Hepatologie und der Immunologie weiterzubilden, wie auch meine Fähigkeiten im Labor auszubauen. Ich möchte mich für diese wundervolle Möglichkeit als auch für die gute Betreuung zunächst einmal bei meiner Doktormutter Frau Prof. Dr. Gisa Tiegs bedanken. Ich hatte eine schöne, aufregende und sehr lehrreiche Zeit, welche außerdem mit sehr viel Spaß verbunden war. Vielen Dank dafür, dass ich an diesem Forschungsprojekt und in Ihrer Arbeitsgruppe arbeiten durfte. Mein weiterer Dank gilt natürlich Prof. Dr. Thomas Dobner, der sich bereit erklärt hatte mein Zweitgutachten zu übernehmen! Danke für Ihre Zeit und Ihr Interesse!

Anschließend geht mein Dank an Dr. Roja Barikbin, die als Projektleiterin für mich zuständig war und mich in die Thematik als auch in die Methodik eingeführt hatte. Trotz ihrer Führung genoss ich einige Freiheiten, die mir erlaubte, eigene Entscheidungen zu treffen und mich eigenständig weiterzuentwickeln. Danke!

Nachfolgend möchte ich mich herzlichst bei unseren technischen Assistenten Carsten und Elena bedanken, die mir immer mit Rat und Tat zur Seite standen und ihr Bestmögliches getan haben um mir die Arbeit zu erleichtern. Sei es um 7 Uhr anfangen, PCR machen, oder sei es Schneiden und Färbungen machen, ich konnte mich immer auf euch verlassen. Vielen Dank für eure Unterstützung!

Auch möchte ich mich bei Dr. Katrin Neumann bedanken, vor allem für ihre Mithilfe bei der Publikation dieser Arbeit. Darüber hinaus möchte mich sehr für ihre Bereitschaft, meine Doktorarbeit zu korrigieren, bedanken. Das war mir eine große Hilfe!

Ein sehr großer Dank geht zudem an meine Kollegen, die immer für mich da waren und mich in allen Aspekten unterstützt haben und auch für ein entspanntes Arbeitsklima gesorgt haben. Ich konnte mich immer auf euch verlassen und hatte auch sehr viel Spaß mit euch. DANKE! Ihr habt mir eine unglaubliche Zeit in Hamburg ermöglicht und unvergessliche Erinnerungen gegeben! Ich hatte eine wundervolle Zeit! Insbesondere möchte ich mich bei Birgit Schiller, Laura Berkhout und Mareike Kellerer für die Unterstützung, für die Geduld und für die Unterhaltung bedanken!

Nachfolgend möchte ich mich auch bei den Kooperationspartnern und speziell bei dem Leberteam für die gute Zusammenarbeit bedanken!

Mein größter Dank geht natürlich an meine Eltern, ohne deren aufopferungsvollen Einsatz, ich nicht in dieser Position wäre, ihr seid die Besten! Auch möchte ich mich bei meinen Schwestern Pira und Thivy und meinem Mann (Raguraj) für die Unterstützung und das Vertrauen bedanken. Ich liebe euch!

Danke an ALLE!

Eidesstattliche Versicherung

Hiermit erkläre ich an Eides statt, dass die die vorliegende Dissertation selbst verfasst und keine anderen als die angegebenen Quellen und Hilfsmittel benutzt habe.

Hamburg, 22.06.2020 

Ort und Datum Gevitha Ananthavettivelu

Confirmation of linguistic accuracy by a native speaker

Charlotte Hamway
Sigmund-Freud Straße 103
60435 Frankfurt am Main

Studienbüro
z.H. Frau Petra Ziemer
MIN Fakultät
Universität Hamburg
Biozentrum Klein Flottbek
Ohnhorststraße 18
22609 Hamburg

27.Oktober.2019

Sehr geehrte Damen und Herren,

Ich, Charlotte Hamway, bestätige als englische Muttersprachlerin, dass die von Frau Gevitha Ananthavettivelu mit dem Titel „The role of IFN in the immune pathogenesis of primary sclerosing cholangitis" vorgelegte Dissertation in korrektem Englisch geschrieben ist.

Mit freundlichen Grüßen

Charlotte Hamway